Mercury isotopes in a forested ecosystem: Implications for air-surface exchange dynamics and the global mercury cycle

Jason D. Demers,[1] Joel D. Blum,[1] and Donald R. Zak[2]

Received 18 September 2011; revised 12 December 2012; accepted 21 December 2012; published 20 March 2013.

[1] Forests mediate the biogeochemical cycling of mercury (Hg) between the atmosphere and terrestrial ecosystems; however, there remain many gaps in our understanding of these processes. Our objectives in this study were to characterize Hg isotopic composition within forests, and use natural abundance stable Hg isotopes to track sources and reveal mechanisms underlying the cycling of Hg. We quantified the stable Hg isotopic composition of foliage, forest floor, mineral soil, precipitation, and total gaseous mercury ($THg_{(g)}$) in the atmosphere and in evasion from soil, in 10-year-old aspen forests at the Rhinelander FACE experiment in northeastern Wisconsin, USA. The effect of increased atmospheric CO_2 and O_3 concentrations on Hg isotopic composition was small relative to differences among forest ecosystem components. Precipitation samples had δ^{202}Hg values of −0.74 to 0.06‰ and Δ^{199}Hg values of 0.16 to 0.82‰. Atmospheric $THg_{(g)}$ had δ^{202}Hg values of 0.48 to 0.93‰ and Δ^{199}Hg values of −0.21 to −0.15‰. Uptake of $THg_{(g)}$ by foliage resulted in a large (−2.89‰) shift in δ^{202}Hg values; foliage displayed δ^{202}Hg values of −2.53 to −1.89‰ and Δ^{199}Hg values of −0.37 to −0.23‰. Forest floor samples had δ^{202}Hg values of −1.88 to −1.22‰ and Δ^{199}Hg values of −0.22 to −0.14‰. Mercury isotopes distinguished geogenic sources of Hg and atmospheric derived sources of Hg in soil, and showed that precipitation Hg only accounted for ~16% of atmospheric Hg inputs. The isotopic composition of Hg evasion from the forest floor was similar to atmospheric $THg_{(g)}$; however, there were systematic differences in δ^{202}Hg values and MIF of even isotopes (Δ^{200}Hg and Δ^{204}Hg). Mercury evasion from the forest floor may have arisen from air-surface exchange of atmospheric $THg_{(g)}$, but was not the emission of legacy Hg from soils, nor re-emission of wet-deposition. This implies that there was net atmospheric $THg_{(g)}$ deposition to the forest soils. Furthermore, MDF of Hg isotopes during foliar uptake and air-surface exchange of atmospheric $THg_{(g)}$ resulted in the release of Hg with very positive δ^{202}Hg values to the atmosphere, which is key information for modeling the isotopic balance of the global mercury cycle, and may indicate a shorter residence time than previously recognized for the atmospheric mercury pool.

Citation: Demers, J. D., J. D. Blum, and D. R. Zak (2013), Mercury isotopes in a forested ecosystem: implications for air-surface exchange dynamics and the global mercury cycle, *Global Biogeochem. Cycles*, *27*, 222–238, doi:10.1002/gbc.20021.

1. Introduction

[2] Natural abundance mercury stable isotope measurements have become a valuable tool for examining the biogeochemical cycling of mercury in the natural environment. Mercury cycling between the atmosphere, biosphere, and lithosphere involves active redox chemistry, phase transformations (including a volatile form), formation of covalent bonds, and biological incorporation. There is a mass difference of ~4% among the seven stable isotopes of mercury (196, 198, 199, 200, 201, 202, 204 amu) that result in significant variations in isotopic composition in natural environmental samples. Because mercury is fractionated in the environment, isotopic signatures can be utilized to both trace sources and identify mechanisms of transformation. For example, mercury isotopes have been employed successfully to trace sources of mercury accumulating in biota, soils, and sediments [*Estrade et al.*, 2010; *Senn et al.*, 2010; *Estrade et al.*, 2011; *Gehrke et al.*, 2011a, 2011b] as well as to identify processes responsible for the transport, transformation, and fate of mercury in natural ecosystems [e.g., *Bergquist and Blum*,

All supporting itnformation may be found in the online version of this article.

[1]Department of Earth and Environmental Sciences, University of Michigan, Ann Arbor, Michigan, USA.
[2]School of Natural Resources and Environment, University of Michigan, Ann Arbor, Michigan, USA.

Corresponding author: J. D. Demers, University of Michigan, Department of Earth and Environmental Sciences, Ann Arbor, MI 48109, USA. (jdemers@umich.edu)

0886-6236/13/10.1002/gbc.20021

2007; *Jackson et al.*, 2008; *Sherman et al.*, 2009; *Sherman et al.*, 2010]. However, there are still significant uncertainties regarding the cycling of mercury at global, regional, and ecosystem scales.

[3] The biogeochemical cycling of mercury in forested ecosystems is particularly complex, as forests mediate the deposition of mercury from the atmosphere and influence its ultimate fate in terrestrial ecosystems. Natural and anthropogenic sources of mercury are emitted to the atmosphere as gaseous elemental mercury (GEM, $Hg(0)_{(g)}$), divalent reactive gaseous mercury (RGM, $Hg(II)_{(g)}$), and particulate-bound mercury associated with aerosols (PBM, $Hg_{(p)}$). Research over the last two decades suggests that, once emitted, RGM is quickly stripped from the atmosphere and deposited locally in wet deposition, whereas $Hg_{(p)}$ is transported more regionally, and $Hg(0)_{(g)}$ may be transported more globally before being oxidized to RGM and deposited [*Keeler et al.*, 1995; *Lindberg and Stratton*, 1998; *Schroeder and Munthe*, 1998]. Thus, atmospheric mercury is mostly comprised of $Hg(0)_{(g)}$ (>95%) [e.g., *Lindberg and Stratton*, 1998], and current estimates suggest an atmospheric residence time of ~1 year [*Fitzgerald and Mason*, 1997; *Mason and Sheu*, 2002; *Hedgecock and Pirrone*, 2004; *Gustin et al.*, 2008 and references therein], although evidence of rapid air-surface exchange in the marine boundary layer may imply a shorter average atmospheric residence time [*Hedgecock and Pirrone*, 2004]. GEM is accumulated in foliage, primarily in stomata, where it is retained (likely in oxidized form) and deposited with litterfall [e.g., *Mosbaek et al.*, 1988; *Rea et al.*, 1995; *Rea et al.*, 2001; *St. Louis et al.*, 2001; *Rea et al.*, 2002; *Rutter et al.*, 2011]. RGM and $Hg_{(p)}$ also adsorb to leaf surfaces, where the mercury may either be photo-reduced and re-emitted to the atmosphere [*Graydon et al.*, 2006; *Millhollen et al.*, 2006a; *Mowat et al.*, 2011], or leached by precipitation and deposited with throughfall [e.g., *Iverfeldt*, 1991; *Kolka et al.*, 1999b; *Rea et al.*, 2000, 2001; *Demers et al.*, 2007]. Mercury deposited to the forest floor is largely retained in association with organic matter [e.g., *Meili*, 1991; *Yin et al.*, 1997; *Kolka et al.*, 1999a; *Kolka et al.*, 2001; *Grigal*, 2003], but may also be exported in association with dissolved organic carbon (DOC), leached and deposited in mineral soil horizons or transported to aquatic ecosystems [e.g., *Meili*, 1991; *Mierle and Ingram*, 1991; *Kolka et al.*, 2001; *Shanley et al.*, 2002; *Demers et al.*, 2010; *Dittman et al.*, 2010], or it may be re-emitted from the forest floor to the atmosphere as $Hg(0)_{(g)}$ [e.g., *Carpi and Lindberg*, 1998; *Hintelmann et al.*, 2002; *Kuiken et al.*, 2008a, 2008b; *Graydon et al.*, 2009].

[4] Despite substantial progress in quantifying fluxes and total pools of mercury in forested ecosystems, identifying the sources and tracking the fate of these various fluxes have proven to be more challenging. For example, although we can estimate the relative contribution of individual fluxes to the forest floor (e.g., precipitation, litterfall, throughfall), it is difficult to distinguish the degree to which each of these individual fluxes are retained or lost from the soil mercury pool. Identifying the sources and mechanisms of mercury evasion from the forest floor has been particularly challenging.

[5] Conceptually, there are a number of mercury evasion source pools within the soil environment, including Hg(0) in soil-gas, Hg(0) or Hg(II) in soil solution, and Hg(0) or Hg(II) adsorbed on solid particle surfaces [*Zhang and Lindberg*, 1999]. Physical, chemical, and biological processes that regulate the distribution of Hg(0) and Hg(II) among soil-gas, solution, and particle phases, or that are involved in redox reactions that reduce Hg(II) to Hg(0), may all influence mercury evasion from soils, although biological processes are thought to be relatively slow [*Zhang and Lindberg*, 1999]. The distribution (i.e., the adsorption and desorption) of Hg(0) in the soil environment is thought to be influenced by organic matter, colloidal amorphous oxides, reducible iron and manganese, surface area, and soil moisture (water molecules can displace Hg(0) from mineral soil surfaces) [*Lindberg et al.*, 1999; *Zhang and Lindberg*, 1999]. In acidic soils, adsorption of Hg(II) depends primarily on organic matter, whereas in neutral soils, mineralogic components such as clays and iron and manganese oxides also adsorb mercury, although not as strongly as organic matter [*Schuster*, 1991; *Zhang and Lindberg*, 1999]. Reduction is thought to involve direct photolysis from solutions or surfaces, or result from light-induced reactions involving DOC, Fe(III)-organic acid complexes, metal oxides, and free radicals [*Zhang and Lindberg*, 1999]; however, dark reactions in the presence of organic acids may also reduce mercury [*Zhang and Lindberg*, 1999]. Additionally, Hg(0) dry deposited directly to soil and litter-covered surfaces represents another pool of mercury available for subsequent re-emission and may be particularly important for air-surface exchange dynamics involving background soils (i.e., soils with low concentrations of Hg, ≤ 100 ng/g) [*Zhang et al.*, 2001; *Ericksen et al.*, 2006; *Gustin et al.*, 2006; *Lyman et al.*, 2007; *Xin et al.*, 2007; *Xin and Gustin*, 2007; *Kuiken et al.*, 2008a, 2008b]. Thus, the specific physicochemical characteristics and associated cycling of mercury between reduced and oxidized forms in the soil environment, as well as at the air-soil interface, influence the sources and mechanisms of mercury emission.

[6] Environmental factors also influence the magnitude and dynamics of mercury evasion from soils, with differences in response somewhat dependent on the level of natural or anthropogenic enrichment, parent material and soil type, and importantly, the presence of organic matter. High soil mercury concentrations increase mercury evasion from soils [e.g., *Rasmussen et al.*, 1998; *Gustin et al.*, 2003; *Feng et al.*, 2005], whereas background soil concentrations (≤ 100 ng/g) may not correlate well with emissions [*Nacht and Gustin*, 2004; *Schroeder et al.*, 2005; *Kuiken et al.*, 2008a, 2008b]. Moreover, small amounts of soil organic matter (e.g., as little as 0.1% SOM as fulvic or humic acids) and leaf litter cover strongly inhibit mercury emissions from soil, even in the presence of light [*Engle et al.*, 2006; *Kuiken et al.*, 2008a, 2008b; *Mauclair et al.*, 2008; *Choi and Holsen*, 2009a, 2009b]. Nonetheless, solar radiation is commonly found to increase mercury evasion from enriched, background (≤ 100 ng/g), mineral, and organic soils [e.g., *Carpi and Lindberg*, 1997, 1998; *Gustin et al.*, 2002], although this effect has been difficult to disentangle from air and soil temperature effects, which also correlate with mercury evasion [e.g., *Carpi and Lindberg*, 1998; *Wallschlager et al.*, 1999]. In forests, canopy shading dramatically reduces mercury emissions [e.g., *Carpi and Lindberg*, 1997; *Zhang et al.*, 2001; *Gustin et al.*, 2004; *Kuiken et al.*, 2008b]. Precipitation promotes mercury evasion from soil by both displacing soil air containing Hg(0), as well as displacing Hg(0) bound to mineral surfaces [e.g., *Lindberg et al.*, 1999]. Enriched isotope spike experiments with desert soils and in

boreal forests have shown that a small amount of newly wet-deposited mercury may initially be more available for re-emission than native mercury pools [*Hintelmann et al.*, 2002; *Ericksen et al.*, 2005], although re-emission of a considerable fraction of wet and dry deposited mercury from surface soils may be significantly delayed [e.g., *Xin et al.*, 2007]. Overall, there remains considerable uncertainty in the identification of the available soil mercury pools, the processes responsible for emission and re-emission, and the environmental controls on the magnitude and dynamics of mercury fluxes to the atmosphere.

[7] Elevated atmospheric carbon dioxide (CO_2) and tropospheric ozone (O_3) may alter the biogeochemical cycling of mercury in forested ecosystems. Elevated CO_2 typically stimulates net primary productivity (NPP), increasing both aboveground and belowground biomass production [e.g., *Kubiske et al.*, 1998; *King et al.*, 2005; *Zak et al.*, 2007]; whereas, phytotoxic O_3 typically has the opposite effect [e.g., *Karnosky et al.*, 2003; and references therein]. Because deposition of Hg to forests is greatly enhanced by the forest canopy, elevated CO_2 and/or O_3 induced changes in physiology or leaf biomass could affect deposition of Hg to the forest floor. *Millhollen et al.* [2006b] showed that elevated CO_2 resulted in lower Hg concentrations in foliage of grasses and forbs, suggesting that foliar uptake of Hg was controlled by stomatal conductance, which is typically reduced under elevated CO_2. *Natali et al.* [2008] also observed lower Hg concentrations in foliage and litter exposed to elevated CO_2, but there were no direct effects of CO_2 on litterfall, throughfall, or stemflow inputs in loblolly pine (*Pinus taeda*) and sweetgum (*Liquidambar styraciflua*) forests at the Duke and Oak Ridge FACE (Free-Air CO_2 Enrichment) sites, respectively. Nonetheless, soil mercury concentrations in these forest FACE sites were 30% greater under elevated CO_2, and were correlated with percent soil organic matter (%SOM), suggesting that CO_2-mediated changes in SOM influenced the accumulation of mercury in soils [*Natali et al.*, 2008]. Whereas the Duke and Oak Ridge forest FACE sites demonstrated that elevated CO_2 tends to increase the rate of soil carbon (C) storage, elevated CO_2 at the Rhinelander FACE site did not increase soil C content in any of its three forest communities [*Talhelm et al.*, 2009; and references therein]. However, elevated CO_2 did increase new C in all SOM fractions, and decreased old C in fine particulate organic carbon (fPOC) and mineral-associated organic matter (MAOM), thus favoring C accumulation in less stable pools with more rapid turnover [*Hofmockel et al.*, 2011]. Whereas mechanisms for the augmentation of Hg inputs by changes in forest structure and function seem plausible, significant changes in soil pools due to Hg release dynamics seems less likely, because leaching losses from forest soils are small relative to inputs [e.g., *Demers et al.*, 2007], and Hg evasion from forest soils is typically inhibited by organic matter and leaf litter cover [e.g., *Kuiken et al.*, 2008a, 2008b]. Furthermore, *Grigal* [2003] suggested that increases in the Hg:C ratio of soils resulted from the mineralization of carbon without the concomitant volatilization of associated Hg, and others have shown that Hg content actually increases (on a mass basis) during litter decomposition [*Hall and St. Louis*, 2004; *Demers et al.*, 2007].

[8] In addition to moderating CO_2 responsiveness of forests, O_3 may also have a more direct influence on mercury speciation and deposition. For example, ozone exposure results in formation of antioxidants in leaf tissue [*Karnosky et al.*, 2003], some of which contain reduced sulfur functional groups (e.g., glutathione reductase) that provide additional strong binding sites for the retention of Hg in leaf tissue. Moreover, O_3 promotes the oxidation of GEM ($Hg(0)_{(g)}$) to RGM ($Hg(II)_{(g)}$), increasing Hg solubility and adsorption to surfaces, and resulting in more rapid wet and dry deposition. Thus, the mechanisms by which elevated CO_2 and O_3 may affect the cycling of mercury in forest ecosystems are complex and often opposing in their ultimate effects.

[9] Mercury isotope fractionation, including both mass-dependent and mass-independent fractionation (MDF and MIF), may provide unique insight into the sources, mechanisms, and ultimate fate of mercury cycling in forested ecosystems. Mass-dependent fractionation (MDF) occurs under both kinetic and equilibrium conditions, and results from differences in vibrational energy of molecules relative to isotope nuclear mass, with heavy nuclei having a lower zero-point energy, reacting more slowly, and thus preferentially remaining in the reactant pool [*Bigeleisen and Mayer*, 1947; *Urey*, 1947; *Blum and Bergquist*, 2007; *Buchachenko*, 2009]. Mass-independent fractionation (MIF) is a measure of the deviation from predicted kinetic mass-dependent fractionation. Mass-independent fractionation (MIF) of mercury isotopes is thought to occur due to both the nuclear volume effect (NVE) and the magnetic isotope effect (MIE). However, the nuclear volume effect (NVE), resulting from differences in nuclear radius of different isotopes, is only considered to contribute significantly to overall mercury isotope effects during equilibrium reactions [*Bigeleisen*, 1996; *Schauble*, 2007; *Buchachenko*, 2009; *Estrade et al.*, 2009]. Whereas the NVE is predicted to influence both even and odd isotopes, the MIE only effects odd-mass isotopes and may be either positive or negative in sign. The magnetic isotope effect (MIE) only occurs during kinetic reactions and results in isotopic separation of odd-mass isotopes (which are magnetic) due to the influence of the nuclear magnetic moment on radical pair reactions [*Buchachenko*, 2001; *Berdinskii et al.*, 2004]. Thus, the MIE is thought to be uniquely indicative of spin-selective reactions that are controlled by the magnetic moment of the reactant nuclei, and not by nuclear mass [*Bergquist and Blum*, 2009; *Buchachenko*, 2009].

[10] Observations of fractionation during controlled experiments are useful for interpreting data collected from natural ecosystems. MDF has been observed during microbial reduction, producing elemental mercury enriched in light isotopes [*Kritee et al.*, 2007; *Kritee et al.*, 2008]. Abiotic aqueous reduction of mercury with or without organic acids during light and dark reactions also results in products that are enriched in light isotopes, with the heavy isotopes remaining in reactant solution (+MDF) [*Bergquist and Blum*, 2007; *Zheng et al.*, 2007; *Zheng and Hintelmann*, 2009, 2010a]. Abiotic photochemical reduction additionally results in MIF of the odd isotopes (Δ^{199}Hg and Δ^{201}Hg; see *Methods: Mercury Isotope Analysis* for definition of capital delta notation) [*Bergquist and Blum*, 2007; *Zheng and Hintelmann*, 2009], the sign of which is dependent upon the type of organic ligand involved [*Zheng and Hintelmann*, 2010a]. The Δ^{199}Hg/Δ^{201}Hg ratio produced during MIF by different mechanisms may also be diagnostic of particular

processes. During equilibrium reactions (e.g., during evaporation experiments), MIF occurring due to the NVE was initially estimated to result in a $\Delta^{199}Hg/\Delta^{201}Hg$ ratio of ~2.0 [*Ghosh et al.*, 2008; *Estrade et al.*, 2009]; whereas, more recent studies have refined that ratio to be ~1.6 [*Ghosh et al.*, 2013]. Abiotic non-photochemical reduction of inorganic Hg (II) by dissolved organic matter and stannous chloride due to the NVE results in a $\Delta^{199}Hg/\Delta^{201}Hg$ ratio of 1.5–1.6 [*Zheng and Hintelmann*, 2010b]. During kinetic reactions, MIF occurring due to MIE results in a $\Delta^{199}Hg/\Delta^{201}Hg$ ratio of ~1.0 during reduction of Hg(II) and ~1.3 during degradation of methyl mercury (MeHg) [*Bergquist and Blum*, 2007].

[11] Previous observations of MDF and MIF in natural environmental samples are also useful for putting new observations into context. The mercury isotopic composition of geogenic sources such as rocks and volcanic emissions is characterized by small negative MDF with no significant MIF [*Smith et al.*, 2008; *Zambardi et al.*, 2009]. Background atmospheric wet precipitation samples observed to date have been characterized by near zero MDF with positive MIF [*Gratz et al.*, 2010], whereas background atmospheric $THg_{(g)}$ has displayed positive MDF with slightly negative MIF complementary to that of precipitation [*Gratz et al.*, 2010]. In contrast, coal deposits and organic soils are generally characterized by large negative MDF, and small, mostly negative MIF [e.g., *Biswas et al.*, 2008; *Lefticariu et al.*, 2011; *Sherman et al.*, 2012]. On a mechanistic level, *Sherman et al.* [2010] used the MIF signature and $\Delta^{199}Hg/\Delta^{201}Hg$ ratio of mercury emitted from snow surfaces to lend insight into the processes driving emissions following arctic atmospheric mercury depletion events and to estimate the proportion of Hg re-emitted from the snowpack. Moreover, deposition of mercury from anthropogenic sources has been tracked to lichen and soils based on shifts in MDF in the receiving soils [*Estrade et al.*, 2010, 2011], various sources of mercury contamination to San Francisco Bay sediments have been identified and tracked into fish based on isotopic composition [*Gehrke et al.*, 2011a, 2011b], and the origin of Gulf of Mexico fish methyl mercury has been distinguished between near-shore and deep-ocean sources based on MIF and MDF signatures [*Senn et al.*, 2010]. Thus, natural abundance Hg isotopes may provide a means of tracking sources and differentiating processes that have given rise to Hg isotopic composition in forested ecosystems, and have the potential to reveal new insights into unresolved issues regarding the biogeochemical cycling of Hg (as discussed in *Introduction*).

[12] In this study, our objectives were to: (1) characterize the isotopic composition of fluxes and pools of mercury in a forested ecosystem; (2) use natural abundance stable mercury isotopes to track sources of mercury as they are biogeochemically cycled within the forested ecosystem; (3) advance our understanding of mechanisms underlying the biogeochemical cycling of mercury within the forested ecosystem; and (4) begin to quantify the effect of elevated CO_2 and elevated O_3 on the mercury isotopic composition of those fluxes, pools, and processes.

2. Methods

2.1. Site Description

[13] The Rhinelander Free-Air CO_2 and O_3 Enrichment (FACE) site is located in northeastern Wisconsin, USA (49º, 40.5'N; 89º, 37.5'E; 490 m elevation). The Rhinelander FACE study was designed to test the response of a northern hardwood ecosystem to elevated CO_2, O_3, and the interaction of elevated CO_2 and O_3, during regeneration from seedlings to mature trees [*Dickson et al.*, 2000]. The site consists of twelve rings (each 30 m diameter), spaced 100 m apart to minimize treatment effects between rings, in a full-factorial design with three ambient rings, three elevated CO_2 rings, three elevated O_3 rings, and three elevated $CO_2 + O_3$ rings distributed among 3 blocks from north to south. Blocks were based on slight differences in soils across the study area [*Dickson et al.*, 2000]. Target concentration for the CO_2 treatment was 560 μmol/mol (~200 μmol/mol above ambient 1996 levels); O_3 treatment consisted of daily episodic exposure following a diurnal profile, the maximum of which was adjusted based on daily meteorological conditions and ranged from 50–100 nmol/mol [*Dickson et al.*, 2000; and references therein]. Detailed information regarding the Rhinelander FACE study design and execution has been published previously [*Dickson et al.*, 2000].

[14] The Rhinelander FACE rings were established on coarse sandy loam soils (mixed, frigid, coarse loamy Alfic Haplorthod) that were under prior agricultural management. The sandy loam surface soil (~15 cm) grades into an argillic horizon (Bt horizon; clay loam from ~15 to 45 cm depth) that is underlain by a C horizon composed of sandy loam, stratified sand, and gravel. Soil properties differed little across the site (see *Dickson et al.*, 2000 for a complete analysis of soil within each ring). In June 1997, each Rhinelander FACE ring was divided into three sections and planted with three tree species common to northern hardwood forests of the Great Lakes region: trembling aspen (*Populous tremuloides* Michx), paper birch [*Betula papyrifera* Marsh.), and sugar maple [*Acer saccharum* Marsh.). Half of each ring was planted with 5 different aspen genotypes (8 L, 43E, 216, 259, 271) with varying tolerance to O_3 [*Karnosky et al.*, 1996b] and varying response to CO_2 enrichment [*Kubiske et al.*, 1998]; the remaining two ring quarters were planted with an aspen and sugar maple community, or an aspen and paper birch community. Stem density (10,000 stems/ha) was within the range of naturally occurring ~10-year-old aspen stands [*Fraser et al.*, 2006; *Mulak et al.*, 2006]. Canopy closure was complete in all aspen-only ring sections beginning in 2003 [*Zak et al.*, 2007].

2.2. Sample Collection and Processing

[15] In this study, we focused on foliage, forest floor, mineral soil, and soil evasion $THg_{(g)}$ measurements from the aspen-only community, with foliage mercury isotopes characterized for only the aspen 216 clone, which displays a moderate response to CO_2 and O_3 [*Karnosky et al.*, 1996a, 1996b]. Atmospheric $THg_{(g)}$ samples were taken at the top of the canopy at plot center within ambient treatment rings. Precipitation samples were collected in an open field nearby.

2.2.1. Foliage, Forest Floor, and Mineral Soils

[16] Foliage, forest floor, and mineral soil samples were collected during August 2008. Foliage was collected along profiles through the canopy (top, >75% of total canopy height; upper-middle, 50–75%; lower-middle, 25–50%; bottom, < 25%) in each ambient and treatment ring section; canopy heights were ~8–10 m. Forest floor samples (4 per ring, 26 cm × 26 cm quadrats, 0.0676 m^2) were collected

randomly from each ambient and treatment ring section. After removal of the forest floor, mineral soil cores (0–20 cm) from each ring section were composited into a single sample. Additional mineral soil samples collected in 2007 at depths of 0–5 cm and 5–10 cm were also analyzed to assess differences in mercury concentration and isotopic composition along the soil depth profile in ambient rings. Foliage, forest floor, and mineral soil samples were stored in plastic bags and frozen until processed. Foliage consisted of new leaves, including petioles, and was dried at 60 °C. Mineral soil samples (0–20 cm cores) were also dried at 60 °C, whereas mineral soil samples from 2007 (0–5 cm, 5–10 cm cores) were freeze-dried. Forest floor samples were also freeze-dried. All samples were ground in an alumina grinding cylinder in a mixer mill; grinding blanks using Ottawa sand (baked at 750 °C) before and between forest floor sample sets showed no detectable contamination or carry-over. Organic matter content (%) of forest floor and mineral soil samples was determined by loss on ignition (LOI).

2.2.2. Atmospheric $THg_{(g)}$

[17] Total gaseous mercury ($THg_{(g)}$ = GEM + RGM) was collected from the atmosphere at the top of the canopy in ambient rings simultaneously with $THg_{(g)}$ evading from the forest floor in the ambient, elevated CO_2, and elevated O_3 rings during June 2009, well after the forest canopy had fully developed. At the time of $THg_{(g)}$ sampling, the forest floor predominantly consisted of the foliage cohort sampled one year prior. In order to collect enough mercury for isotopic analysis of atmospheric $THg_{(g)}$ at these sites, air was drawn through eight gold-coated bead traps deployed in parallel via a PVC manifold at a target rate of 1.8 L/min per trap over 24–72 hours (timing varied due to weather, samplers were not operated during precipitation events) (modified from *Gratz et al.*, 2010; *Sherman et al.*, 2010). The inlet to each trap utilized a pre-baked quartz-fiber pre-filter. The performance of gold-coated bead traps was verified with spikes of 10 ng Hg (NIST SRM 3133), blanked, and then blank-checked prior to use. Mean recovery of spikes was 91.1% (n = 23, 5.7%, 1SD); maximum composite blank-check per set of 8 traps was ≤ 0.3 ng.

2.2.3. Soil Evasion $THg_{(g)}$

[18] Soil evasion $THg_{(g)}$ samples were collected in the same manner as atmospheric $THg_{(g)}$ samples, except that each sample collection trap was connected to a flux chamber. Because the primary goal of our soil evasion collection was to determine the isotopic composition of emitted mercury (rather than quantify fluxes), it was necessary to isolate the evasion flux from ambient atmospheric $THg_{(g)}$; thus, our flux chambers differed in design from dynamic flux chambers typically used for evasion flux measurements. Flux chambers consisted of sturdy polycarbonate boxes (50 cm x 29 cm x 14.5 cm), with a footprint surface area of 0.15 m^2. Although polycarbonate is less transmissive of UV light than Teflon (in particular, UV-B light < 320 nm wavelength; *Carpi et al.*, 2007), and some studies have shown reduced soil mercury emissions with chambers made of polycarbonate materials [e.g., *Carpi et al.*, 2007], numerous studies have also shown no consistent difference or that responses to natural light are muted but not eliminated [e.g., *Gustin et al.*, 1999; *Wallschlager et al.*, 1999; *Engle et al.*, 2001; *Lindberg et al.*, 2002]. The inlet to the flux chamber was a gold-coated bead trap mounted in one end-wall that acted as an ambient atmospheric $THg_{(g)}$ filter. The outlet from the flux chamber was mounted in the opposite end-wall, and was connected by Teflon tubing to the quartz-fiber pre-filter of the sample collection trap. Chambers were installed over intact forest floor by setting each chamber in place, carefully cutting around the perimeter, and then pushing the chamber 3.5 cm into the soil. As the chamber was pushed into place, its inward sloping walls promoted a firm connection with undisturbed soil. Additionally, chambers were pegged into place and the forest floor and soil around the outer perimeter was firmly pressed back into place around each installed chamber. The flushing rate based on dry test meter (DTM) measurements was 2.2 L/min on average, with a chamber volume turnover rate of 6.6 minutes (calculated from data in Supporting Table S1), both of which are within the range used for dynamic flux chambers in other studies [e.g., *Carpi and Lindberg*, 1998; *Lindberg et al.*, 1999; *Wallschlager et al.*, 1999; *Gustin et al.*, 2002; *Lindberg et al.*, 2002; *Ericksen et al.*, 2006; *Gustin et al.*, 2006; *Kuiken et al.*, 2008b] and are similar to the ideal high flushing rates suggested by *Lindberg et al.* [2002]. In block 1 and block 2, soil evasion measurements were made as described; for comparison, in block 3, the effect of soil evasion on isotopic composition of ambient atmospheric $THg_{(g)}$ at the forest floor was assessed by placing the inlet tubes, without chambers, within 1 cm of forest floor.

2.2.4. Precipitation

[19] Precipitation samples were collected on an event basis during late summer and fall 2010 using manual collection methods developed by the University of Michigan Air Quality Laboratory [*Landis and Keeler*, 1997], hereafter referred to as manual event precipitation. In short, clean manual single-event sampling trains were deployed prior to forecasted precipitation and retrieved upon completion of an event [after *Landis and Keeler*, 1997]. All parts of the sampling train were cleaned by submersion in a 10% HNO_3 bath at 75 °C for at least 12 hours; subsequently, sample bottles were filled with 5% BrCl and allowed to soak for at least 24 hours, and rinsed with Hg-free de-ionized water. All sample bottles were deployed with a 20 ml aliquot of 1% HCl (trace metal grade, verified to be Hg-free) in order to preserve samples in the field and prevent volatile losses [*Landis and Keeler*, 1997]. After collection, samples were brought to 0.5% HCl by volume, further oxidized with 1% BrCl by volume (verified to be Hg-free), and allowed to react in a dark cold-room at 4 °C for at least 1 month prior to analysis for mercury concentration.

2.3. Mercury Concentration Analysis, Calculations, and QA/QC

[20] Mercury concentrations were measured using standard methods and samples were analyzed in batches with quality control that included independent primary and secondary standards, continuing calibration verification standards, continuing calibration blanks, matrix spike recovery tests, analysis of duplicate or triplicate samples, reference materials, and equipment and procedural blanks. Foliage, forest floor, and mineral soil sub-samples (~ 50 mg) were analyzed for concentration of total mercury (THg, all forms of mercury) by combustion at 850 °C and analysis by cold-vapor atomic absorption spectrometry (CVAAS; MA-2000, Nippon Instruments). The THg concentration of manual event precipitation samples was determined following a method modified from EPA Method 1631 [USEPA, 1998]

using an automated CVAAS (MA-2000 with liquid delivery system; Nippon Instruments). After the atmospheric and evasion $THg_{(g)}$ samples on each set of eight gold-coated bead traps had been desorbed into a 1% $KMnO_4$ trapping solution (see *Methods: Sample Preparation for Isotopic Analysis*), a small aliquot was analyzed for concentration and the total quantity of mercury collected was calculated. Detailed procedures and assessment of QA/QC for these measurements are available (see *Supporting Information: Methods (unabridged)*).

2.4. Sample Preparation for Isotope Analysis

2.4.1. Offline Combustion of Foliage, Forest Floor, and Soil

[21] Foliage and soils were prepared by two-stage combustion with inline trapping of released mercury in order to remove matrix interferences and concentrate mercury for isotopic analysis. This apparatus and method was based on a previous study [*Smith et al.*, 2005] that was modified for lower Hg concentration samples by *Biswas et al.* [2008]. In this study, we further modified the procedure to allow for slow, controlled, complete combustion of organic samples (i.e., vegetation) while preventing the condensation of organic combustion residues in the furnace system upstream of the trapping media. Reduced mercury released by combustion was trapped with an oxidizing solution of 1% $KMnO_4$ (w/w) in 10% sulfuric acid (v/v) (hereafter, referred to as 1% $KMnO_4$). The mercury concentration of a small aliquot of 1% $KMnO_4$ solution was measured in order to determine full procedural recovery, as well as to allow matching of standard and sample concentrations for isotope analysis.

[22] Offline combustion performance was monitored with procedural blanks, combustion of reference materials, and by the percent recovery of samples based on independent sample mercury concentration analyses (*see Methods: Mercury Concentration Analysis, Calculations, and QCQA*). Procedural blanks were performed at a frequency of at least every 8 samples; average procedural blanks resulted in 0.009 ng/g ($\pm$ 0.008, 1SD, $n = 9$) 1% $KMnO_4$ solutions prior to transfer and 0.027 ng/g ($\pm$ 0.013, 1SD, $n = 9$) subsequent to transfer. We combusted NIST SRM 1515 (Apple Leaves, 44 $\pm$ 4 ng/g) with recovery ranging from 88.5 to 99.3% (mean = 96.6 $\pm$ 3.6%, 1SD, $n = 9$); we also combusted several aliquots of BCR 062 (Olive Leaves, 280 $\pm$ 20 ng/g) with recovery ranging from 95.1 to 105.7% (mean = 102.9 $\pm$ 6.9%, 1SD, $n = 3$; Supporting Table S2). Mean percent recovery for samples of foliage was 92.7% ($\pm$ 3.2%, 1SD, $n = 12$), for forest floor was 97.9% ($\pm$ 5.9%, 1SD, $n = 18$), and for mineral soil was 94.3% ($\pm$ 2.7%, 1SD, $n = 9$).

2.4.2. Desorption of Atmospheric and Evasion $THg_{(g)}$

[23] Atmospheric and soil evasion $THg_{(g)}$ samples collected on gold-coated bead traps in the field were concentrated into a 1% $KMnO_4$ solution for isotope analysis through a multi-step process, modified from the procedure used by *Gratz et al.* [2010] in order to increase efficiency, and decrease the procedural blank (see *Supporting Information: Methods (unabridged)*). The 1% $KMnO_4$ trap solution was then measured for mercury concentration, and subsequently transferred and concentrated into a secondary 1% $KMnO_4$ trap solution resulting in final concentrations ranging from 2.9–4.4 ng/g for isotope analysis, following the same procedure as outlined for the offline combustion trap solutions (*see Methods: Offline Combustion of Foliage, Forest Floor, and Soils*). The performance of the desorption procedure was monitored with procedural blanks and procedural standards analyzed in the same manner as samples. Procedural blanks and procedural standards began with sets of eight blanked gold-coated bead traps; traps for the procedural standards were loaded with 30 and 80 ng Hg (NIST SRM 3133) per set to represent the range of $THg_{(g)}$ collected. Average procedural blanks were 0.55 ng ($\pm$ 0.40, 1SD, $n = 3$). Recovery of procedural standards using NIST SRM 3133 ranged from 89.2 – 94.2% (mean = 91.1 $\pm$ 1.9%, 1SD, $n = 6$), and were not significantly fractionated relative to NIST SRM 3133 bracketing standards (Supporting Table S2).

2.4.3. Purging and Trapping of Precipitation Samples

[24] Mercury in manual event precipitation samples was purged and trapped into 1% $KMnO_4$ solution for isotope analysis. Up to 1 L of previously acidified and oxidized precipitation was weighed into a clean 2 L borosilicate glass media bottle, combining precipitation samples from all three collection funnels for each event. Samples were treated with 300 μl of 30% hydroxylamine hydrochloride to destroy free halogens, capped tightly, and allowed to react for 1 hour. A clean Teflon stir bar was added to the 2 L media bottle, and a three-port Teflon transfer cap was securely attached. The first port was reserved for the delivery of 100 ml of 5% $SnCl_2$ via peristaltic pump without compromising the closed system. The second port was used to draw gold-filtered clean-room air into the sample solution through a sparger with a medium frit in order to purge reduced mercury into the headspace of the 2 L media bottle. The third port was an outlet tube that connected to another sparger and medium frit within a narrow elongated borosilicate glass trap (~2 cm diameter, ~30 cm height) containing 5.5 g of 1% $KMnO_4$ trapping solution. The sidearm of the transfer cap of the 1% $KMnO_4$ trap was connected in series to a flow meter and a diaphragm vacuum pump that was used to achieve a flow of ~ 0.7 L/min through the system. After flows were established, the 5% $SnCl_2$ was dripped into the sample solution at a rate of ~10 ml/min, and sample solutions were purged for 3 hours.

[25] To quantify purge and trap recovery, the mercury concentration of the 1% $KMnO_4$ trap solution was determined as outlined for the offline combustion trap solutions (*see Methods: Offline Combustion of Foliage, Forest Floor, and Soils*), scaled to total precipitation volume, and compared to total mass of mercury within the three collection funnel samples from each event. The final concentration of Hg in precipitation samples in 1% $KMnO_4$ for isotope analysis was 1.1–1.7 ng/g. We monitored the performance of the purge and trap system with procedural blanks (mean = 0.012 $\pm$ 0.005 ng/g, 1SD, $n = 3$) and procedural standards. Procedural standards consisted of 12 ng of Hg (NIST SRM 3133) split between one, two, or three 2 L media bottles, and diluted to 1 L with Hg-free de-ionized water acidified and oxidized following the same procedure as that for sample solutions. Procedural standards were then purged, trapped, and analyzed in the same manner as samples. Procedural standard recovery was 90.2 $\pm$ 2.0% (1SD, $n = 3$); there was no apparent difference among samples purged singly, or in multiple sequential aliquots; purge and trap procedural standards using NIST SRM 3133 were not significantly fractionated relative to NIST SRM 3133 bracketing standards (Supporting Table S2).

2.5. Mercury Isotope Analysis

2.5.1. MC-ICP-MS

[26] Mercury from natural environmental samples was concentrated into a 1% $KMnO_4$ solution and analyzed for isotopic composition with a multiple collector inductively coupled plasma mass spectrometer (MC-ICP-MS; Nu Instruments) using continuous flow cold vapor generation with Sn(II) reduction [*Lauretta et al.*, 2001; *Blum and Bergquist*, 2007]. We employed an arrangement of faraday cups that allows for simultaneous collection of masses 196, 198, 199, 200, 201, 202, 203, 204, 205, and 206. Instrumental bias was corrected using an internal standard (NIST SRM 997, $^{205}Tl/^{203}Tl$ ratio of 2.38714) and strict sample-standard bracketing with NIST SRM 3133 Hg standard. Analyses were run at 1–5 ng/g Hg, with standard concentrations matched to within 5% of sample concentrations. Isobaric interferences from ^{204}Pb were monitored to allow correction using mass 206; however, interferences from ^{204}Pb were always negligible. On-peak zero corrections were applied to all masses.

[27] We report isotopic compositions as permil (‰) deviations from the average of NIST SRM 3133 bracketing standards using delta notation:

$$\delta^{xxx}\mathrm{Hg}\ (‰) = \left\{ \left[\left({}^{xxx}\mathrm{Hg}/{}^{198}\mathrm{Hg} \right)_{\mathrm{unknown}} / \left({}^{xxx}\mathrm{Hg}/{}^{198}\mathrm{Hg} \right)_{\mathrm{NIST\ SRM\ 3133}} \right] - 1 \right\} \times 1000 \quad (1)$$

where xxx is the mass of each mercury isotope between ^{199}Hg and ^{204}Hg. We use $\delta^{202}Hg$ to assess MDF. MIF is reported as the deviation of the isotope ratio from the theoretically predicted values based on the kinetic mass-dependent fractionation law and measured $\delta^{202}Hg$ [*Blum and Bergquist*, 2007]. MIF is reported in "capital delta" notation ($\Delta^{xxx}Hg$) in units of permil (‰) (Equation 2), and is well approximated for small ranges in delta values (≤ 10 ‰) by Equation 3:

$$\Delta^{xxx}\mathrm{Hg}\ (‰) = 1000\, x\, (\{\ln[(\delta^{xxx}\mathrm{Hg}/1000) + 1]\} - \beta\, x\, \{\ln[(\delta^{202}\mathrm{Hg}/1000) + 1]\} \quad (2)$$

$$\Delta^{xxx}\mathrm{Hg}\ (‰) \approx \delta^{xxx}\mathrm{Hg} - (\delta^{202}\mathrm{Hg}\, x\, \beta) \quad (3)$$

where xxx is the mass of each mercury isotope 199, 200, 201, 204 and β is a constant (0.252, 0.502. 0.752, 1.492, respectively; *Blum and Bergquist*, 2007).

2.5.2. Reporting Analytical Uncertainty

[28] We characterized the uncertainty of mercury isotope measurements using a secondary standard that is widely distributed (UM-Almaden), as well as with procedural standards for each natural environmental matrix [*Blum and Bergquist*, 2007]. To characterize the reproducibility of the mass spectrometry, we measured the isotopic composition of UM-Almaden several times (3–7x) at each analytical concentration within each analytical session. The 2SD uncertainty was then generated from the average of session averages for each delta value; there was no difference in the reproducibility for concentrations ranging from 1–5 ng/g during the analytical sessions reported in this study. For the procedural standard of each sample matrix type (as described in *Methods: Sample Preparation for Isotope Analysis*), we calculated uncertainty as 2SE of the average of session averages. We represent the uncertainty of samples with the uncertainty (2SE) of associated procedural standards; however, where the 2SE of procedural standards was less than the 2SD of UM-Almaden, we instead represent sample uncertainty using UM-Almaden. The uncertainty associated with the isotopic composition of UM-Almaden, procedural standards and reference materials, and environmental samples are presented in Supporting Tables S2–S7.

3. Results and Discussion

[29] We first present mercury concentrations and isotopic values of individual forest ecosystem pools and fluxes. Subsequently, we discuss the patterns and processes of the biogeochemical cycling of mercury that interrelates these pools and fluxes within the forested ecosystem, as informed by natural abundance mercury isotope composition and fractionation. However, before interrelating the isotopic data from these ecosystem components, it is important to consider the temporal variability represented by the samples. The foliage, forest floor, and mineral soil mercury pools were all sampled in late August 2008. The foliage was sampled near the end of the growing season, as it approached maximum mercury content, and was therefore a temporally integrated sample of foliar mercury. The forest floor predominantly consisted of ~1–2 years of decomposing litter inputs, and mineral soil pools also reflect a long, temporally integrated time horizon. Total gaseous mercury ($THg_{(g)}$) in the atmosphere and from soil flux chambers was sampled simultaneously in June 2009, and thus could be directly compared. Moreover, in June 2009 when we sampled $THg_{(g)}$ evasion, the forest floor predominantly consisted of foliage deposited as litterfall from the previous year; that is, the same foliage we sampled in August 2008. Thus, we were able to use Hg isotope data to assess whether the source of $THg_{(g)}$ evasion was derived directly from the soils or the forest floor. Total gaseous mercury ($THg_{(g)}$), and precipitation samples collected in late summer and fall 2010, were the least temporally integrated measures of Hg isotope composition. However, as we report herein, atmospheric $THg_{(g)}$ and precipitation sampled in this study were found to be isotopically similar to measurements made in 2007, 2008, and 2009 in a non-urban-industrial region of the Upper Midwest [*Gratz et al.*, 2010]. Importantly, all of these $THg_{(g)}$ and precipitation measurements made in the Upper Midwest region display an isotopic composition that is distinct from all other components of the forested ecosystem (see Figure 1). Thus, our study provides integration and assessment of the temporal variability of isotopic composition for each ecosystem component, and therefore establishes a reasonable framework within which to track sources and assess mechanisms underlying the biogeochemical cycling of mercury using natural abundance stable isotope techniques.

3.1. Mercury Concentrations and Isotopic Composition in the Forest Ecosystem

[30] Mercury isotopic composition varied widely between different pools and fluxes within the forested ecosystem, an essential attribute enabling the use of isotopic techniques to study the biogeochemical cycling of mercury. The $\delta^{202}Hg$ values ranged from −2.53‰ in foliage to +1.60‰ in $THg_{(g)}$ evaded from the forest floor, and $\Delta^{199}Hg$ values ranged from −0.37‰ in foliage to +0.82‰ in precipitation (Figure 1).

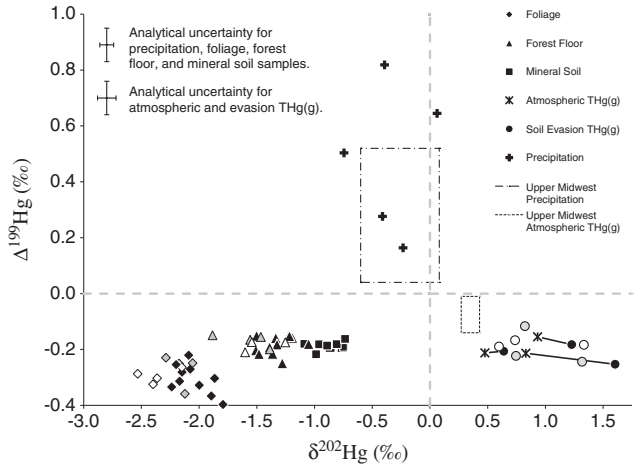

Figure 1. Mercury isotopic composition of forest ecosystem components in aspen-only ring sections at the Rhinelander FACE site in northeastern Wisconsin, USA. MDF is assessed with δ^{202}Hg in permil (‰); MIF is shown by Δ^{199}Hg (‰). Gray dashed lines show zero-values for δ^{202}Hg and Δ^{199}Hg. Measured forest ecosystem components include foliage, forest floor, mineral soil, total gaseous mercury ($THg_{(g)}$) in atmospheric samples above the canopy and from soil evasion, and precipitation; individual field replicates are shown; see *Methods* for additional details about each component characterized and determination of uncertainty. Black lines are used to connect atmospheric $THg_{(g)}$ to soil evasion $THg_{(g)}$ collected simultaneously in each of the ambient plots. Treatment data are shown for foliage, forest floor, and soil evasion $THg_{(g)}$ (ambient = black; elevated CO_2 = gray, elevated O_3 = white). Dashed-boxes show the range of mercury isotopic composition in precipitation and atmospheric $THg_{(g)}$ measured in rural areas of the Upper Midwest region [*Gratz et al.*, 2010].

The mercury concentration, isotopic composition, and uncertainty associated with isotope ratio measurements for UM-Almaden, procedural standards and reference materials, and all samples are summarized in Supporting Tables S2–S7.

3.1.1. Foliage

[31] Aspen 216 foliage mercury concentration increased ~2-fold from the top of the canopy to the bottom of the canopy within all treatments in aspen-only ring sections of Block 1 (Supporting Table S3 and Figure 2a); however, the isotopic composition of aspen 216 foliage was similar within each canopy profile (Figure 2b). This suggests that despite strong mercury concentration gradients through the forest canopy, the source and mechanism of mercury uptake by foliage did not appear to differ with canopy position.

[32] We observed a significant treatment effect on mercury isotopic composition in aspen 216 foliage within the Block 1 aspen-only ring sections of the Rhinelander FACE experiment. Foliar exposure to both elevated CO_2 and elevated O_3 drove δ^{202}Hg to more negative values (mean δ^{202}Hg = −2.03‰ ± 0.11‰ for ambient treatment foliage, $n = 4$; −2.16‰ ± 0.10‰ for elevated CO_2 treatment foliage, $n = 4$; and −2.36‰ ± 0.16‰ for O_3 treatment foliage, $n = 4$; Figure 3). However, only the elevated O_3 effect on δ^{202}Hg was statistically different from the ambient treatment ($p = 0.012$ for ambient versus elevated O_3, $p = 0.113$ for ambient versus elevated CO_2, with Tukey adjustment for degrees of freedom). We did not measure mercury isotopes in foliage from the elevated $CO_2 + O_3$ interaction treatment, nor from Block 2 or Block 3. Thus, we acknowledge that our approach lacks true replication, and that our inferences are limited to Block 1 of Rhinelander FACE. Furthermore, we characterized mercury isotopes in foliage of only the aspen 216 clone, and it is known that different aspen clones had different foliar growth responses to Rhinelander FACE treatments [*Karnosky et al.*, 1996a, 1996b; *Karnosky et al.*, 2003; *Zak et al.*, 2007]. Thus, these results indicating elevated O_3 treatment effects on foliage mercury isotope composition should be considered preliminary, and warrant further study. Overall, foliage mercury isotopic composition was characterized by the most negative δ^{202}Hg values (−1.79‰ to −2.53‰) and the most negative MIF for ^{199}Hg (Δ^{199}Hg = −0.22‰ to −0.40‰) relative to all other measured components of the forested ecosystem (Figure 1).

3.1.2. Forest Floor and Mineral Soil

[33] Forest floor mercury δ^{202}Hg values and MIF (δ^{202}Hg = −1.05‰ to −1.88‰ ; Δ^{199}Hg = −0.15‰ to −0.25‰) were less negative than observed for foliage (Figure 1 and Supporting Tables S3 and S4). This was due, in part, to natural physical mixing (e.g., bioturbation) of the forest floor with

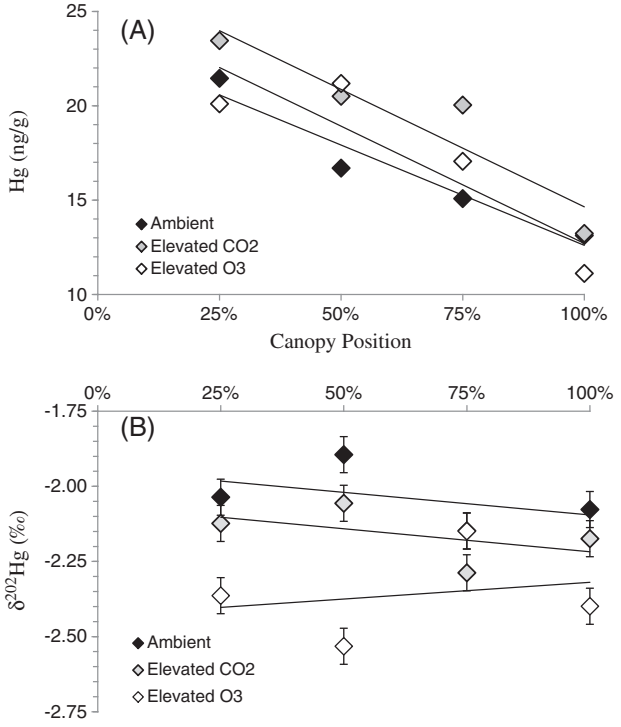

Figure 2. Relationship between canopy position and (A) foliage mercury concentration (ng/g), and (B) δ^{202}Hg in permil (‰) in the aspen-only ring sections at the Rhinelander FACE site in northeastern Wisconsin, USA. Canopy profiles of the aspen 216 foliage from Block-1 ambient, elevated CO_2, and elevated O_3 treatment plots are shown. Canopy position is represented as percentage of total canopy height (~8–10 m), such that 100% is at the top of the canopy. Error bars in (B) show the analytical uncertainty of δ^{202}Hg values (see *Methods: Reporting Analytical Uncertainty* for details).

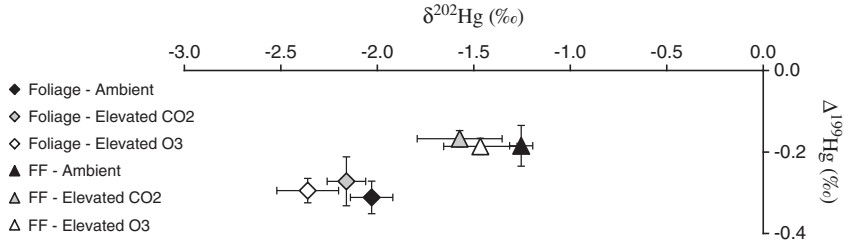

Figure 3. Treatment effect of elevated CO_2 and elevated O_3 on the isotopic composition of mercury in the forest floor (FF), and aspen 216 foliage of the aspen-only ring sections of Block-1 at the Rhinelander FACE site in northeastern Wisconsin, USA. Here we show aspen ring section means for forest floor (FF), and for foliage from canopy profiles of the aspen 216 clone ($n = 4$ reps per ring section; error bars are 1SD of field replicates).

underlying mineral soil. The underlying mineral soil had negative MIF similar to that observed for the forest floor (Δ^{199}Hg = −0.16‰ to −0.22‰), but had more positive δ^{202}Hg values (−1.09‰ to −0.74‰) corresponding to a decrease in organic matter content (Figure 1, Figure 4b, and Supporting Table S5). Thus, the treatment effect on the mercury isotopic composition in foliage did not translate into statistically significant treatment effects within the forest floor ($p = 0.069$; Figure 3), in part due to the mixing of decaying foliage with underlying mineral soil. Furthermore, we only measured mercury isotope ratios in the aspen 216 clone, whereas forest floor mercury isotope composition was influenced by litterfall from all aspen genotypes.

[34] Mineral soil horizon mercury concentrations (23.8 to 37.0 ng/g) were similar to those measured in the Upper Midwest region in previous studies [*Nater and Grigal*, 1992]. The contribution of mineral soil to the forest floor samples (mineral soil % = 100% − organic matter %) was well correlated with forest floor δ^{202}Hg values (Figure 4b; $y = 0.012x - 2.051$; 0.001 and 0.064, 1SE for slope and intercept, respectively; $p < 0.0001$ for both slope and intercept parameters). Extrapolating this relationship to 0% organic matter results in an estimation of a δ^{202}Hg value for pure mineral soil (−0.84‰ ± 0.03‰, 1SE) that approaches δ^{202}Hg values reported for geogenic mercury from a variety of crustal source rocks [e.g., −0.62‰ ± 0.20‰, *Smith et al.*, 2008]. Extrapolating to 100% organic matter results in a δ^{202}Hg estimate (−2.05‰ ± 0.06‰, 1SE) that is within error of the average δ^{202}Hg value of foliage (mean δ^{202}Hg = −2.14‰ ± 0.19‰, 1SD, $n = 18$). These results suggest that mercury associated with organic matter in the soil mostly originates from the decomposition of foliage, which is consistent with mass balance studies demonstrating the importance of litterfall inputs to soil Hg pools [e.g., *St. Louis et al.*, 2001], and that the mercury isotopic composition of the foliage does not significantly change during the decomposition process. This makes intuitive sense, in that mercury must be lost in order for fractionation to occur. Little dissolved organic carbon is lost via leaching in this ecosystem as carbon is primarily lost to the atmosphere via respiration [*Zak et al.*, 2007], and mercury is concentrated in recalcitrant residual soil organic matter [*Grigal*, 2003]. Thus, forest floor mercury isotope data are consistent with our conceptual understanding, and provide us with a tool for differentiating between geogenic mercury soil pools, and that which has been recently deposited from the atmosphere and incorporated into organic matter.

3.1.3. Precipitation

[35] Precipitation displayed mostly small negative δ^{202}Hg values (0.06‰ to −0.74‰), in contrast with the foliage, forest floor, and mineral soil δ^{202}Hg values, and was the only ecosystem component in this study that showed positive MIF (Δ^{199}Hg = 0.16‰ to 0.82‰; Supporting Table S6 and Figure 1). The most negative δ^{202}Hg value in precipitation coincided with an unusual large rain event with southerly flow from urban-industrial areas to the south, and may be indicative of mercury contributed from regional anthropogenic emissions such as combustion of coal [*Gratz et al.*, 2010; *Sherman et al.*, 2012]. The range of Δ^{199}Hg values in the manual single-event-based precipitation samples in this study was slightly more positive than measured previously for automated multi-event-based wet-only

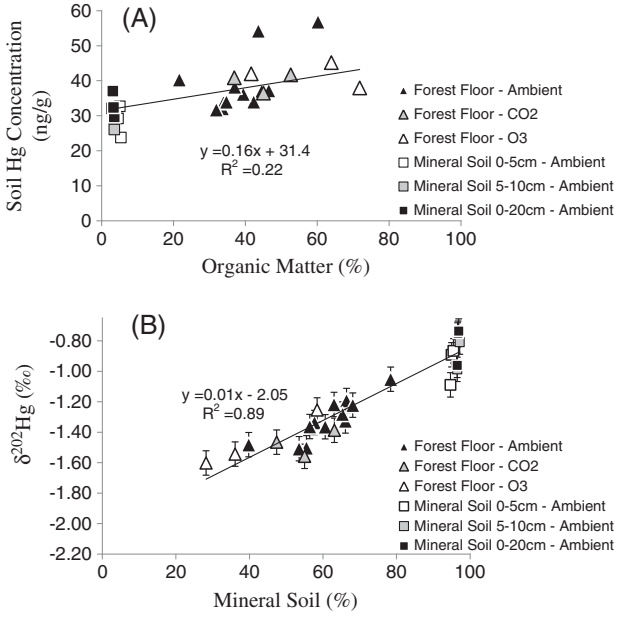

Figure 4. Relationship between (A) organic matter (%) and mercury concentration (ng/g), and (B) mineral soil (%) and δ^{202}Hg in permil (‰) of forest floor and mineral soils in the aspen-only ring sections of ambient, elevated CO_2, and elevated O_3 treatment rings at the Rhinelander FACE site in northeastern Wisconsin, USA. Individual field replicates are shown; error bars in (B) represent the analytical uncertainty of δ^{202}Hg values (see *Methods: Reporting Analytical Uncertainty* for details).

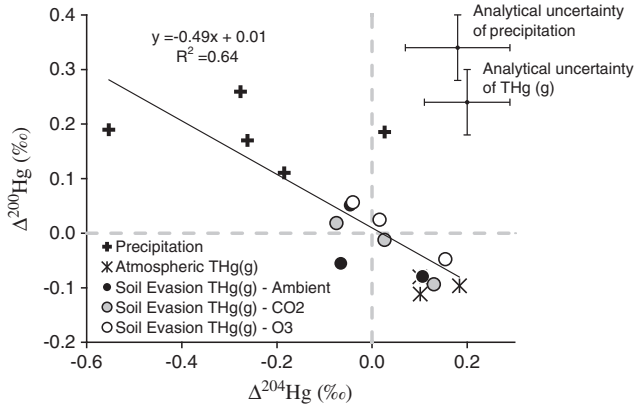

Figure 5. Mass-independent fractionation of even isotopes (Δ^{200}Hg and Δ^{204}Hg) in precipitation, and atmospheric and soil evasion $THg_{(g)}$ at the Rhinelander FACE site in northeastern Wisconsin, USA. Individual field replicates are shown; see *Methods* for additional details about each component characterized and determination of analytical uncertainty.

precipitation in the Upper Midwest (Δ^{199}Hg = 0.04‰ to 0.52‰; Figure 1; *Gratz et al.*, 2010]; mixing of multiple events and multiple sources may limit the observation of more extreme isotopic values. Overall, the isotopic composition of mercury in the manual single-event-based precipitation samples in this study compared well with measurements made previously for multi-event-based precipitation samples from other non-urban-industrial sites in the Upper Midwest (Figure 1), an indication that we have a reasonably good estimate of mercury isotopic composition in precipitation in this region.

3.1.4. Atmospheric and Soil Evasion $THg_{(g)}$

[36] Total gaseous Hg ($THg_{(g)}$) in the atmosphere above the forest canopy and evaded from forest soils were both characterized by significant positive δ^{202}Hg values and significant negative MIF (Figure 1 and Supporting Table S7). The isotopic composition of atmospheric $THg_{(g)}$ in this study (δ^{202}Hg = 0.48‰ to 0.93‰, Δ^{199}Hg = −0.15‰ to −0.21‰) also compared well with, but was slightly more extreme than, the isotopic composition of atmospheric $THg_{(g)}$ sampled from other non-urban-industrial regions of the Upper Midwest (mean δ^{202}Hg = 0.33‰ ± 0.08‰, 1SD; mean Δ^{199}Hg = −0.10‰ ± 0.05‰, 1SD), and was quite distinct from $THg_{(g)}$ measurements taken in Chicago or originating from more urban-industrial areas (mean δ^{202}Hg = −0.49‰ ± 0.13‰, 1SD; mean Δ^{199}Hg = −0.08‰ ± 0.19‰, 1SD) [*Gratz et al.*, 2010]. This suggests that during our atmospheric $THg_{(g)}$ sampling period, the rurally located Rhinelander FACE site received air masses containing a limited amount of mercury emitted from local and regional anthropogenic sources.

[37] Total gaseous Hg ($THg_{(g)}$) evaded from the forest floor displayed a larger and more positive range of δ^{202}Hg values (δ^{202}Hg = 0.60‰ to 1.60‰) than did the atmospheric $THg_{(g)}$ from above the forest canopy, whereas the negative MIF values were similar (Δ^{199}Hg = −0.12‰ to −0.25‰) (Figure 1 and Supporting Table S7). This δ^{202}Hg value of 1.60‰ represents one of the most positive δ^{202}Hg values measured previously in any natural environmental sample (other than hydrothermal deposits, *Smith et al.*, 2005), and shows that mercury evasion from soil in this study released Hg with very positive δ^{202}Hg to the global mercury reservoir.

3.2. Mass-Independent Fractionation of Even Isotopes

[38] Recently, *Gratz et al.* [2010] reported significant positive MIF of ^{200}Hg in precipitation (mean Δ^{200}Hg = 0.16‰ ± 0.06‰, 1SD) coupled with slightly negative MIF of ^{200}Hg in atmospheric $THg_{(g)}$ (mean Δ^{200}Hg = −0.05‰ ± 0.04‰, 1SD). In this study, we similarly observed significant positive MIF in ^{200}Hg of precipitation (mean Δ^{200}Hg = 0.18‰ ± 0.05‰, 1SD) and significant negative MIF of ^{200}Hg in atmospheric $THg_{(g)}$ (Δ^{200}Hg = −0.10‰ ± 0.02‰, 1SD; Supporting Tables S6, and S7). A linear regression of Δ^{199}Hg versus Δ^{200}Hg in precipitation and atmospheric $THg_{(g)}$ in this study yielded a slope of 2.39 ± 0.47 (r^2 = 0.81, p = 0.0023, n = 8), which was similar to the slope of 1.87 ± 0.40 (r^2 = 0.80, $p < 0.001$, n = 27) determined for this relationship by *Gratz et al.* [2010].

[39] We also observed negative MIF of ^{204}Hg that was complementary to the Δ^{200}Hg values in our precipitation samples (mean Δ^{204}Hg = −0.25‰ ± 0.21‰, 1SD), and positive MIF of ^{204}Hg that was complementary to Δ^{200}Hg values in our atmospheric $THg_{(g)}$ samples (mean Δ^{204}Hg = 0.13‰ ± 0.05‰, 1SD; Supporting Tables S6, and S7). In contrast with precipitation and atmospheric $THg_{(g)}$, the MIF of ^{200}Hg and ^{204}Hg in $THg_{(g)}$ evaded from the forest floor was indistinguishable from zero (mean Δ^{200}Hg = 0.01‰ ± 0.04‰, 1SD; mean Δ^{204}Hg = −0.03‰ ± 0.04‰, 1SD) (Supporting Table S7 and Figure 5). Note that the chamberless evasion samples taken within 1 cm of the forest floor in Block 3 showed MIF of even isotopes similar to atmospheric $THg_{(g)}$ samples. The linear regression of Δ^{200}Hg versus Δ^{204}Hg in precipitation, atmospheric $THg_{(g)}$, and soil evasion $THg_{(g)}$ had a slope of −0.49 ± 0.10 (r^2 = 0.63, $p < 0.0001$, n = 17; Figure 5). Observations of small, yet significant, MIF of ^{204}Hg and the phenomenon of complementary MIF of ^{200}Hg and ^{204}Hg have not been reported in previous studies. There is no evidence that observed MIF of ^{200}Hg and ^{204}Hg are the result of instrumental or procedural artifacts; UM-Almaden, procedural standards, and reference materials did not show MIF of even isotopes (Supporting Table S2). *Gratz et al.* [2010] speculated that MIF of ^{200}Hg may result from nuclear volume effects or photochemical self-shielding. Recently, *Chen et al.* [2012] hypothesized that Δ^{200}Hg anomalies were produced in the atmosphere, likely derived from redox reactions transforming Hg(0) to Hg(II) followed by scavenging onto droplets or particles during specific oxidation reactions, such as those involving ozone and sunlight, or halogen enriched solid surfaces. We also can only speculate, and do not have a clear explanation for MIF of ^{200}Hg and ^{204}Hg, nor their apparently complementary behavior among precipitation and atmospheric mercury or within individual pools.

3.3. Influence of Photochemical Processes on the Environmental Cycling of Hg

[40] When all precipitation, $THg_{(g)}$, foliage, forest floor, and mineral soil samples are assessed in terms of their Δ^{199}Hg/Δ^{201}Hg ratio, the slope of the regression is close to a slope of 1.0 (0.96 ± 0.05, 1SE, Figure 6). This corresponds

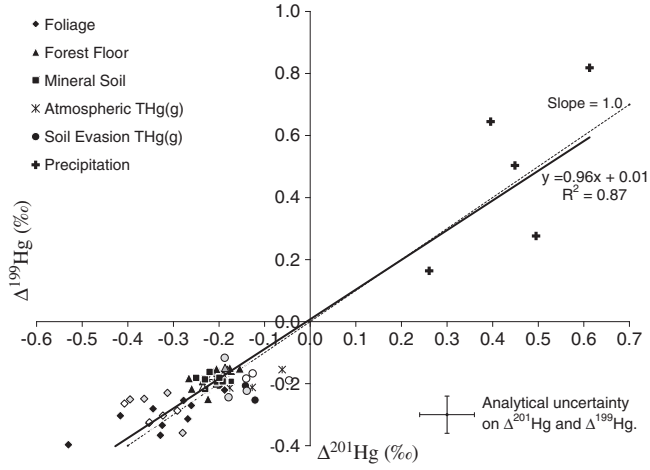

Figure 6. Relationship between Δ^{201}Hg and Δ^{199}Hg in foliage, forest floor, mineral soil, atmospheric and soil evasion $THg_{(g)}$, and precipitation at the Rhinelander FACE site in northeastern Wisconsin, USA. Individual field replicates are shown; see *Methods* for additional details about each component characterized and determination of analytical uncertainty. Treatment data are shown for foliage, forest floor, and soil evasion $THg_{(g)}$ (ambient = black, elevated CO_2 = gray, elevated O_3 = white).

to the $\Delta^{199}Hg/\Delta^{201}Hg$ ratio resulting from MIF during photochemical reduction of mercury from aqueous solutions in the presence of dissolved organic carbon as measured by Berquist and Blum (2007). This finding is consistent with previous work demonstrating that photochemical processes are important in the environmental cycling of mercury [*Amyot et al.*, 1994; *Sellers et al.*, 1996; *Carpi and Lindberg*, 1997, 1998; *Zhang and Lindberg*, 1999; *Gustin et al.*, 2002; *Graydon et al.*, 2006]. However, because MIF signatures are conserved during subsequent processes involving only MDF, this overall relationship does not necessarily reveal where in the cycling of mercury that photochemistry is imparting the observed MIF. Moreover, upon closer inspection, not all of the components of the forested ecosystem have $\Delta^{199}Hg/\Delta^{201}Hg$ ratios that fit the overall relationship. Whereas the majority of data are within analytical uncertainty of the 1:1 line, other data appear to deviate from the 1:1 line by more than the analytical uncertainty; in particular, some of the precipitation data, atmospheric $THg_{(g)}$, and soil evasion $THg_{(g)}$. We speculate that this may be due to a decoupling of the reactants and products of the photochemical reduction reactions responsible for generating the $\Delta^{199}Hg/\Delta^{201}Hg$ ratio. That is, precipitation and $THg_{(g)}$ samples were not collected simultaneously, whereas foliage and forest floor samples are temporally integrated measures. For example, other studies have shown data with $\Delta^{199}Hg/\Delta^{201}Hg$ slopes with non-zero intercepts [*Point et al.*, 2011], and this type of shift could produce the scatter we observe in our data.

3.4. Biogeochemical Cycling of Hg in Forest Ecosystems: An Isotope-Based Perspective

3.4.1. Fractionation During Foliar Uptake of $THg_{(g)}$

[41] We observed a large mass dependent fractionation (MDF) of mercury between atmospheric $THg_{(g)}$ pools and the foliage (mean shift in δ^{202}Hg of −2.89‰) (Figure 1). This represents one of the largest fractionations of mercury measured between two ecosystem components in natural environmental samples, and proceeds in the expected direction of kinetic MDF, as the lighter isotopes pass to the products (i.e., binding within foliage) while the heavier isotopes remain in the reactant (i.e., atmospheric $THg_{(g)}$). Thus, we can infer that the atmospheric $THg_{(g)}$ is chemically binding with components of the foliage and not simply undergoing physical deposition to the surface, although some amount of particulate mercury may also be incorporated. We also observed a slight negative MIF of mercury isotopes between the atmospheric $THg_{(g)}$ pool and the foliage, with a shift in mean Δ^{199}Hg from −0.19‰ (± 0.03‰, 1SD) to −0.29‰ (± 0.06‰, 1SD). This could be due to the influence of the isotopic composition of deposited particulate-bound Hg; however, we did not isolate and characterize particulate-bound Hg. Alternatively, this MIF may arise from volatilization of Hg already bound with the foliage, which would be consistent with the photochemical reduction of Hg(II) in aqueous solutions of low molecular weight organic compounds with sulfur-containing ligands [*Zheng and Hintelmann*, 2010a]. However, the effect of more complex molecules and mixtures of differing ligands (especially ligands containing reduced N) on MIF needs to be further assessed. Overall, the observed direction of mercury isotope fractionation in this study lends support to previous findings that suggest mercury in foliage is bound predominantly within stomatal cavities [e.g., *Rutter et al.*, 2011] in association with abundant sulfur (and nitrogen) containing enzymes, rather than on leaf surfaces where structural components such as cutin are dominated by carboxylic ligands [*Buchanan et al.*, 2000]. However, because our approach using the isotopic fractionation of mercury during the uptake and re-emission of $THg_{(g)}$ by foliage shows the balance of all co-occurring processes, these findings cannot entirely rule out the possibility that non-stomatal pathways may contribute to some fraction of total mercury deposition to foliage [e.g., *Stamenkovic and Gustin*, 2009; *Converse et al.*, 2010].

3.4.2. Sources of Mercury Contributing to the Forest Floor

[42] Forest floor mercury isotope values can be explained by a mixture of mercury originating from the foliage, underlying mineral soil, and precipitation. We used a mixing model based on average mercury isotopic values (δ^{202}Hg and Δ^{199}Hg) from each source in aspen-only ambient rings to estimate that forest floor mercury was comprised of ~42% from foliage, ~50% from soil, and ~8% directly from precipitation. From this, we calculate that ~84% of total atmospheric inputs are delivered to the forest floor associated with foliage (i.e., litterfall) and only ~16% of inputs are delivered to the forest floor directly from precipitation. This is a somewhat smaller contribution of mercury from precipitation than expected, as previous studies suggest that mercury inputs to the forest floor in deciduous and mixed deciduous-coniferous forests are split more evenly between litterfall (~60%) and throughfall (~40%) [*Lindberg*, 1996; *Rea et al.*, 1996; *Grigal et al.*, 2000; *St. Louis et al.*, 2001; *Demers et al.*, 2007]. This discrepancy may arise, in part, because we did not characterize the isotopic composition of throughfall mercury. Throughfall contributions relative to direct precipitation range from <100% to >200%, with lower throughfall contributions tending to occur in deciduous forests in more rural regions. Also, isotope spike

experiments have shown that some precipitation mercury deposited to leaf surfaces may be rapidly photoreduced and re-emitted to the atmosphere, while a portion may be retained on foliage and deposited with litterfall [*Hintelmann et al.*, 2002; *Graydon et al.*, 2006; *Mowat et al.*, 2011]. Together, these observations suggest that wash-off may contribute nearly double the amount of mercury contributed by direct precipitation to this forest, and that wash-off would be isotopically similar to foliage-bound Hg. Although this is somewhat speculative, it highlights the potential usefulness of isotopes in distinguishing between wet and dry deposition sources of mercury.

3.4.3. Source and Mechanism of Mercury Evasion From the Forest Floor

[43] The isotopic composition of $THg_{(g)}$ evading from the forest floor that was measured in this study was similar to that measured for atmospheric $THg_{(g)}$, but with some subtle differences. In paired simultaneous measurements, $THg_{(g)}$ evading from soils had more positive δ^{202}Hg values than atmospheric $THg_{(g)}$; a paired t-test indicated marginal significance that the mean difference was greater than zero (0.41 ± 0.18‰, 1SE; $t = 2.22$, $p = 0.078$, $n = 3$; PROC TTEST PAIRED, SAS 2009). Based on expectations for kinetic isotope fractionation, air-surface exchange of atmospheric $THg_{(g)}$ with organic surfaces would be expected to result in the observed positive shift in δ^{202}Hg; that is, as ambient air moves through the soil or across the soil surface, lighter mercury isotopes would preferentially adsorb or be oxidized, thus leaving the ambient air mass enriched in heavier isotopes which are then measured as mercury evading from the soil environment. This is not unlike ion exchange column experiments in which the resin becomes enriched in light isotopes, although this is presumably the result of equilibrium fractionation [*Wiederhold et al.*, 2010]. This effect of air-surface exchange is also similar to the fractionation of atmospheric $THg_{(g)}$ upon foliar uptake observed in this study. This mechanism of fractionation between atmospheric and soil evasion $THg_{(g)}$ requires that some portion of atmospheric $THg_{(g)}$ is transferred to the soil, and this is consistent with the decrease in $THg_{(g)}$ concentration between atmospheric $THg_{(g)}$ (1.04 ± 0.05 ng/m^3, 1SD, $n = 3$) and soil evasion $THg_{(g)}$ (0.73 ± 0.18 ng/m^3, 1SD, $n = 9$). Decreases in concentration were found to be significantly different from zero when paired simultaneous measurements were compared [$t = 4.61$, $p = 0.022$, $n = 3$; PROC TTEST PAIRED, SAS 2009). It is possible that our flux chamber design could have induced a slight negative pressure within the chamber (see *Methods: Soil Evasion $THg_{(g)}$*), which could have increased the rate at which $THg_{(g)}$ moved laterally through the surrounding soil environment. Such a phenomenon could have increased the proportion of the evasion flux that originated from atmospheric and soil gas $THg_{(g)}$, thereby influencing the observed isotopic composition of evasion. However, if $THg_{(g)}$ were to pass more rapidly through the soil environment, this would be expected to decrease the fraction of $THg_{(g)}$ oxidized during transit, which would diminish (not enhance) the observed positive shift in δ^{202}Hg values derived from these sources of evasion. Nevertheless, note that for both δ^{202}Hg values and mercury concentrations, our results were consistent regardless of whether soil evasion measurements were made with flux chambers (as in block 1 and block 2), or by chamberless collections of $THg_{(g)}$ within 1 cm of the forest floor (as in block 3). Overall, our data imply that under the sampling conditions we employed, the source of $THg_{(g)}$ evading from soils was derived from the interaction of atmospheric $THg_{(g)}$ with the soil environment, as atmospheric $THg_{(g)}$ passed across or through the soil ecosystem.

[44] The mercury isotopic composition of $THg_{(g)}$ evaded from the soil environment in this study could not have arisen from the bulk forest floor or mineral soil, nor from re-emission of recent wet deposition, based on known mechanisms of mercury isotope fractionation. In previous studies that did not employ mercury isotopes, a commonly invoked mechanism for mercury evasion from forest soils has been photoreduction and volatilization. Photoreduction and volatilization of mercury from aqueous solutions with or without DOC would result in typical kinetic MDF with the reactants becoming enriched in the heavier isotopes, and the products becoming enriched in the lighter isotopes [*Bergquist and Blum*, 2007; *Zheng et al.*, 2007; *Zheng and Hintelmann*, 2009, 2010a]. Additionally, photoreduction results in the MIF of odd isotopes (i.e., ^{199}Hg and ^{201}Hg) [*Bergquist and Blum*, 2007; *Zheng et al.*, 2007; *Zheng and Hintelmann*, 2009, 2010a]. In contrast, mercury sampled from evasion chambers in this study had a much more positive δ^{202}Hg value than the bulk forest floor or the underlying mineral soil, and we did not observe MIF in evasion relative to the forest floor and underlying mineral soil Hg pools (Figure 1). Thus, the mercury isotopic composition of evaded $THg_{(g)}$ observed in this study could not have originated from photoreduction and volatilization of mercury from the bulk forest floor or underlying mineral soil.

[45] It might be argued that $THg_{(g)}$ evaded from soils originates from the bulk forest floor or underlying soil mercury pool through biological reduction of mercury that results in MDF, but not MIF. MIF arises from only a small number of reactions (mostly involving photochemistry), and isotopic signatures imparted by MIF are expected to be conserved during subsequent processes that involve MDF alone and limited mixing of sources [*Bergquist and Blum*, 2009]. Mass dependent fractionation of mercury during biologically mediated reduction to $Hg(0)_{(g)}$ has been demonstrated to occur without significant MIF [e.g., *Kritee et al.*, 2007; *Kritee et al.*, 2008; *Kritee et al.*, 2009]. Thus far, microbiologically mediated reduction has always resulted in the reactants (i.e., the substrate) becoming heavier (more positive), and the products (i.e., $Hg(0)_{(g)}$) becoming lighter (more negative) with respect to δ^{202}Hg values, which is consistent with kinetic mass-dependent fractionation. However, our results showed the opposite, that $THg_{(g)}$ sampled from evasion chambers had δ^{202}Hg values that were significantly more positive than either the forest floor or the underlying mineral soil substrate. Thus, it also does not appear to be possible for the evaded $THg_{(g)}$ in this study to be the result of microbiologically mediated reduction of mercury from the bulk forest floor or underlying mineral soil.

[46] Recent studies have also suggested that wet deposition of mercury may be re-emitted from foliar and soil surfaces to the atmosphere. Using an ecosystem isotope spike experiment, *Hintelmann et al.* [2002] demonstrated that 4–13% of ^{202}Hg applied to boreal forest ground vegetation volatilized back to the atmosphere, with an initial large flux immediately following the spike application that decreased

rapidly (within minutes to hours), suggesting that recent wet deposition was more readily volatilized than old mercury previously bound with vegetation and soil. Isotope spikes have also been used to demonstate that both Hg(II) and MeHg can be rapidly re-emitted from foliar surfaces subsequent to deposition [*Graydon et al.*, 2006; *Mowat et al.*, 2011]. All of these studies suggested that this process of rapid re-emission likely accounts for only a small fraction of deposited mercury. Thus, it is consistent that the isotopic composition of $THg_{(g)}$ in the atmosphere and evading from the forest floor in this study suggests that re-emission of wet-deposited mercury was not a dominant process under the environmental conditions we sampled. It should be noted that the polycarbonate chambers used in this study may have diminished (but not eliminated) the potential for photochemical processes to influence the evasion of mercury from soils [e.g., *Gustin et al.*, 1999; *Wallschlager et al.*, 1999; *Engle et al.*, 2001; *Lindberg et al.*, 2002; *Moore and Carpi*, 2005; *Carpi et al.*, 2007; *Choi and Holsen*, 2009b], and that future studies investigating the flux or isotopic signature of mercury evading from soils may benefit from the use of flux chambers constructed of Teflon or quartz materials.

[47] Studies of mercury evasion from forest soils with background mercury concentrations (≤ 100 ng/g) have shown that soil evasion fluxes are extremely low (similar to this study), likely due to high organic matter content, suppression by leaf litter cover, and canopy shading [e.g., *Carpi and Lindberg*, 1998; *Kuiken et al.*, 2008a, 2008b; *Choi and Holsen*, 2009a, 2009b]. It is possible that mercury evading from Hg-contaminated or naturally-Hg-enriched soils (> 100 ng/g), or soils less influenced by organic matter, leaf litter, and canopy shading, may emit $THg_{(g)}$ from soils that originates from sources other than atmospheric $THg_{(g)}$. It is also possible that fractions of the soil ecosystem that we did not characterize may be contributing to measured soil evasion (e.g., soil-gas), and this warrants further investigation. Based on this study, we suggest that natural abundance mercury isotope methods will prove to be a very useful technique for investigating and identifying soil evasion sources in other ecosystems and under various environmental conditions, as it is possible that multiple sources and mechanisms contribute under differing conditions. Nonetheless, according to the mercury isotope data obtained in this study, $THg_{(g)}$ evaded from the soil was not derived from volatilization of significant amounts of legacy mercury from forest soils, nor wet-deposition, but instead represented a more rapid cycling of recent atmospherically derived $THg_{(g)}$ through the forest soil ecosystem.

4. Conclusions and Global Implications

[48] Mercury isotopic composition varied widely within the forested ecosystem, making natural abundance mercury isotope techniques a valuable tool for identifying and tracking sources of mercury, determining its ultimate fate, and suggesting possible mechanisms underlying its biogeochemical cycling. Mercury isotopes can be used to attribute soil mercury between geogenic sources and atmospheric derived mercury that has been incorporated into organic matter, confirming that mercury associated with organic matter in soil is derived from the decomposition of foliage, and showing that the mercury isotopic composition of foliage does not significantly change during the decomposition process. Precipitation mercury represented only a small fraction of atmospheric mercury retained in the forest floor (~16%), further emphasizing the importance of dry deposition of mercury to forested ecosystems. We suggest that future studies may be able to use isotopic measurements of precipitation, dry deposition, and throughfall to better attribute net inputs to forested ecosystems as well as to advance our understanding of wet and dry exchange processes occurring within the forest canopy, over long time scales, and without imposing artificial experimental conditions.

[49] Atmospheric $THg_{(g)}$ was strongly fractionated during uptake by foliage (-2.89‰ for δ^{202}Hg). However, because atmospheric $THg_{(g)}$ and soil evasion $THg_{(g)}$ were similar in mercury isotopic composition (with positive δ^{202}Hg values compared to the very negative δ^{202}Hg values in foliage), we were unable to determine the relative importance of these source(s) of $THg_{(g)}$ accumulating in foliage. The very negative δ^{202}Hg values coupled with small negative MIF in foliage is similar to the mercury isotopic composition of coals [*Biswas et al.*, 2008; *Lefticariu et al.*, 2010, 2011; *Sherman et al.*, 2012], suggesting that the isotopic signature imparted by fractionation upon foliar uptake is at least in part conserved upon coalification. This also implies that the large mass dependent fractionation of atmospheric $THg_{(g)}$ during foliar uptake may be important for understanding the isotopic balance of the global mercury cycle. Moreover, the small MIF signature in foliage is indicative of deposition and re-emission dynamics, and this may represent the terrestrial equivalent of the rapid cycling of mercury observed between the atmosphere and the ocean in the marine boundary layer [*Hedgecock and Pirrone*, 2004].

[50] The source of $THg_{(g)}$ evading from forest soils in this study appeared to be derived from the interaction of atmospheric $THg_{(g)}$ with the soil environment. It is possible that $THg_{(g)}$ evading from Hg-contaminated or naturally-Hg-enriched soils (≥ 100 ng/g), or soils less influenced by organic matter, leaf litter, and canopy shading, may emit $THg_{(g)}$ from soils that originates from sources other than atmospheric $THg_{(g)}$. It is also possible that fractions of the soil ecosystem that we did not characterize in isolation may be contributing to measured soil evasion (e.g., soil gas), and this warrants further investigation. Nonetheless, according to the mercury isotope data obtained in this study, $THg_{(g)}$ evaded from the soil did not represent the emission of legacy mercury from the bulk forest floor, underlying mineral soils, nor the re-emission of recent wet-deposition; but instead, represented a more rapid cycling of $THg_{(g)}$ through the forest soil ecosystem that results in net deposition of $THg_{(g)}$ to the soil ecosystem. If these results can be generalized to all forested ecosystems with background soil mercury levels, then this implies that reductions in anthropogenic emissions to the atmosphere that reduce atmospheric mercury concentrations should also decrease measured rates of soil mercury evasion from background soils of terrestrial ecosystems.

[51] Air-surface exchange of mercury in terrestrial ecosystems, along with air-sea exchange of mercury in the marine boundary layer [e.g., *Mason and Sheu*, 2002; *Hedgecock and Pirrone*, 2004], is important for understanding global mercury cycling and the dynamics of the global atmospheric mercury pool. In this study, we showed that atmospheric $THg_{(g)}$ fractionates during foliar uptake

(−2.89‰ shift in δ^{202}Hg) and during interaction with soil surfaces (0.41‰ shift in δ^{202}Hg), both resulting in the release of Hg with very positive δ^{202}Hg values to the global mercury reservoir. Other air-surface exchange processes in terrestrial ecosystems, such as with lichen [e.g., *Carignan et al.*, 2009; *Sonke et al.*, 2011; *Blum et al.*, 2012] and peat substrates [*Shi et al.*, 2011] also result in surfaces that are enriched in lighter isotopes and atmospheric mercury that is progressively enriched in heavier isotopes. Additionally, we also observed small MIF of Hg associated with foliage (similar to that in lichen), demonstrating that fractionation processes involving photochemical reduction of Hg are prevalent throughout the terrestrial ecosystem, in addition to aquatic ecosystems [e.g., *Bergquist and Blum*, 2007]. *Sonke* [2011] recently utilized MIF signatures alone to model the isotopic balance of the global mercury cycle. Here, by demonstrating strong MDF during air-surface exchange processes with foliage and soil surfaces, this study opens the door for incorporation of MDF into models of the global mercury cycle. It is possible that the growing body of evidence for air-surface exchange of mercury in terrestrial ecosystems, in conjunction with rapid air-sea exchange of mercury in the marine boundary layer [*Hedgecock and Pirrone*, 2004], may point to a shorter residence time of the global atmospheric mercury pool than traditional methods that do not capture the dynamic nature of global mercury cycling. This would require a shift in our conceptual understanding of the global mercury cycle. Rather than mercury being transported globally during a year-long atmospheric residence time, it implies that mercury transport may be shorter range as it is exchanged between the atmosphere and terrestrial (or oceanic) ecosystems. This would not only imply that local and regional emissions sources are important on local and regional scales, but also that the global atmospheric mercury pool should respond rapidly to changes in emissions. Our observations of MDF during air-surface exchange provide a means for incorporating MDF (in addition to MIF) into models that could assess and verify the effects of these dynamic processes on the global cycling of Hg.

[52] **Acknowledgments.** We thank Tim Dvonch, Jim Barres, Lynne Gratz and the late Jerry Keeler of the University of Michigan Air Quality Laboratory for providing and assisting with field sampling equipment. We thank Marcus Johnson, Sara Worsham, Sarah North, and members of the UM Biogeochemistry and Environmental Isotope Geochemistry Laboratory for analytical assistance. We thank Mark Kubiske, JoAnne Lund, and Anita Foss of the U.S. Department of Agriculture Forest Service Institute for Applied Ecosystems Studies (Rhinelander, WI) for the collection of precipitation samples, as well as the members of the Rhinelander FACE project for facilitating site access. This research was supported with funding through the Program for Ecosystem Research, Department of Energy; and by the University of Michigan MacArthur Professorship awarded to J.D. Blum.

References

Amyot, M., G. Mierle, D. R. S. Lean, and D. J. McQueen (1994), Sunlight-induced formation of dissolved gaseous mercury in lake waters, *Environ. Sci. Technol.*, *28*, 2366–2371.

Berdinskii, V. L., L. L. Yasina, and A. L. Buchachenko (2004), The magnetic isotope effect and the separation of isotopes in radical reactions: A theory, *Russ. J. Phys. Chem.*, *78*, 261–264.

Bergquist, B. A., and J. D. Blum (2007), Mass-dependent and -independent fractionation of Hg isotopes by photoreduction in aquatic systems, *Science*, *318*, 417–420.

Bergquist, R. A., and J. D. Blum (2009), The odds and evens of mercury isotopes: applications of mass-dependent and mass-independent isotope fractionation, *Elements*, *5*, 353–357.

Bigeleisen, J. (1996), Nuclear size and shape effects in chemical reactions, isotope chemistry of the heavy elements, *J. Am. Chem. Soc.*, *118*, 3676–3680.

Bigeleisen, J., and M. G. Mayer (1947), Calculation of equilibrium constants for isotopic exchange reactions, *J. Chem. Phys.*, *15*, 261–267.

Biswas, A., J. D. Blum, B. A. Bergquist, G. J. Keeler, and Z. Q. Xie (2008), Natural mercury isotope variation in coal deposits and organic soils, *Environ. Sci. Technol.*, *42*, 8303–8309.

Blum, J. D., and B. A. Bergquist (2007), Reporting of variations in the natural isotopic composition of mercury, *Anal. Bioanal. Chem.*, *388*, 353–359.

Blum, J. D., M. W. Johnson, J. D. Gleason, J. D. Demers, M. S. Landis, and S. Krupa (2012), Mercury concentration and isotopic composition of epiphytic tree lichens in the Athabasca Oil Sands, *in* K. E. Percy, editor. Alberta Oil Sands: Energy, Industry and the Environment, Elsevier, Oxford, UK.

Buchachenko, A. L. (2001), Magnetic isotope effect: nuclear spin control of chemical reactions, *J. Phys. Chem. A*, *105*, 9995–10011.

Buchachenko, A. L. (2009), Mercury isotope effects in the environmental chemistry and biochemistry of mercury-containing compounds, *Russ. Chem. Rev.*, *78*, 319–328.

Buchanan, B. B., W. Gruissem, and R. L. Jones (2000), Biochemistry & molecular biology of plants, *Am. Soc. Plant Biologists*, pp. 507–509.

Carignan, J., N. Estrade, J. E. Sonke, and O. F. X. Donard (2009), Odd isotope deficits in atmospheric Hg measured in lichens, *Environ. Sci. Technol.*, *43*, 5660–5664.

Carpi, A., and S. E. Lindberg (1997), Sunlight-mediated emission of elemental mercury from soil amended with municipal sewage sludge, *Environ. Sci. Technol.*, *31*, 2085–2091.

Carpi, A., and S. E. Lindberg (1998), Application of a teflon (TM) dynamic flux chamber for quantifying soil mercury flux: tests and results over background soil, *Atmos. Environ.*, *32*, 873–882.

Carpi, A., A. Frei, D. Cocris, R. McCloskey, E. Contreras, and K. Ferguson (2007), Analytical artifacts produced by a polycarbonate chamber compared to a teflon chamber for measuring surface mercury fluxes, *Anal. Bioanal. Chem.*, *388*, 361–365.

Chen, J. B., H. Hintelmann, X. B. Feng, and B. Dimock (2012), Unusual fractionation of both odd and even mercury isotopes in precipitation from Peterborough, ON, Canada, *Geochim. Cosmochim. Acta*, *90*, 33–46.

Choi, H. D., and T. M. Holsen (2009a), Gaseous mercury emissions from unsterilized and sterilized soils: the effect of temperature and UV radiation, *Environ. Pollut.*, *157*, 1673–1678.

Choi, H. D., and T. M. Holsen (2009b), Gaseous mercury fluxes from the forest floor of the Adirondacks, *Environ. Pollut.*, *157*, 592–600.

Converse, A. D., A. L. Riscassi, and T. M. Scanlon (2010), Seasonal variability in gaseous mercury fluxes measured in a high-elevation meadow, *Atmos. Environ.*, *44*, 2176–2185.

Demers, J. D., C. T. Driscoll, T. J. Fahey, and J. B. Yavitt (2007), Mercury cycling in litter and soil in different forest types in the Adirondack region, New York, USA, *Ecol. Appl.*, *17*, 1341–1351.

Demers, J. D., C. T. Driscoll, and J. B. Shanley (2010), Mercury mobilization and episodic stream acidification during snowmelt: role of hydrologic flow paths, source areas, and supply of dissolved organic carbon. *Water Resour. Res.*, *46*, W01511, doi:10.1029/2008WR007021.

Dickson, R. E., K. F. Lewin, J. G. Isebrands, M. D. Coleman, W. E. Heilman, D. E. Riemenschneider, J. Sober, G. E. Host, D. R. Zak, K. S. Hendrey, K. S. Pregitzer, and D. F. Karnosky (2000), Forest atmosphere carbon transfer storage-II (FACTS II) - the aspen free air CO_2 and O_3 enrichment (FACE) project: an overview. General technical report NC-214, US Department of agriculture forest service north central experiment station, St Paul, MN.

Dittman, J. A., J. B. Shanley, C. T. Driscoll, G. R. Aiken, A. T. Chalmers, J. E. Towse, and P. Selvendiran (2010), Mercury dynamics in relation to dissolved organic carbon concentration and quality during high flow events in three northeastern US streams, *Water Resour. Res.*, *46*, W07522, doi:10.1029/2009WR008351.

Engle, M. A., M. S. Gustin, D. W. Johnson, J. F. Murphy, W. W. Miller, R. F. Walker, J. Wright, and M. Markee (2006), Mercury distribution in two Sierran forest and one desert sagebrush steppe ecosystems and the effects of fire, *Sci. Total Environ.*, *367*, 222–233.

Engle, M. A., M. S. Gustin, and H. Zhang (2001), Quantifying natural source mercury emissions from the Ivanhoe mining district, north-central Nevada, USA, *Atmos. Environ.*, *35*, 3987–3997.

Ericksen, J. A., M. S. Gustin, S. E. Lindberg, S. D. Olund, and D. P. Krabbenhoft (2005), Assessing the potential for re-emission of mercury deposited in precipitation from arid soils using a stable isotope, *Environ. Sci. Technol.*, *39*, 8001–8007.

Ericksen, J. A., M. S. Gustin, M. Xin, P. J. Weisberg, and G. C. J. Fernandez (2006), Air-soil exchange of mercury from background soils in the United States, *Sci. Total Environ.*, *366*, 851–863.

Estrade, N., J. Carignan, and O. F. X. Donard (2010), Isotope tracing of atmospheric mercury sources in an urban area of northeastern France, *Environ. Sci. Technol.*, *44*, 6062–6067.

Estrade, N., J. Carignan, and O. F. X. Donard (2011), Tracing and quantifying anthropogenic mercury sources in soils of northern France using isotopic Signatures, *Environ. Sci. Technol.*, *45*, 1235–1242.

Estrade, N., J. Carignan, J. E. Sonke, and O. F. X. Donard (2009), Mercury isotope fractionation during liquid-vapor evaporation experiments, *Geochim. Cosmochim. Acta*, *73*, 2693–2711.

Feng, X. B., S. F. Wang, G. A. Qiu, Y. M. Hou, and S. L. Tang (2005), Total gaseous mercury emissions from soil in Guiyang, Guizhou, China, *J. Geophys. Res.-Atmos.*, *110*, D14306, doi:10.1029/2004JD005643.

Fitzgerald, W. F., and R. P. Mason (1997), Biogeochemical cycling of mercury in the marine environment. Pages 53-111 *in* metal ions in biological systems, Vol 34.

Fraser, E. C., S. M. Landhausser, and V. J. Lieffers (2006), Does mechanical site preparation affect trembling aspen density and growth 9-12 years after treatment? *New Forest*, *32*, 299–306.

Gehrke, G. E., J. D. Blum, and M. Marvin-DiPasquale (2011a), Sources of mercury to San Francisco bay surface sediment as revealed by mercury stable isotopes, *Geochim. Cosmochim. Acta*, *75*, 691–705.

Gehrke, G. E., J. D. Blum, D. G. Slotton, and B. K. Greenfield (2011b), Mercury isotopes link mercury in San Francisco bay forage fish to surface Sediments, *Environ. Sci. Technol.*, *45*, 1264–1270.

Ghosh, S., Y. F. Xu, M. Humayun, and L. Odom (2008), Mass-independent fractionation of mercury isotopes in the environment, *Geochem. Geophys. Geosyst.*, *9*, Q03004, doi:10.1029/2007GC001827.

Ghosh, S., E. A. Schauble, G. Couloume, J. D. Blum, and B. A. Bergquist (2013), Estimation of nuclear volume dependent fractionation of mercury isotopes in equilibrium liqui-vapor evaporation experiments, *Chem. Geol. 336*, 5–12.

Gratz, L. E., G. J. Keeler, J. D. Blum, and L. S. Sherman (2010), Isotopic composition and fractionation of mercury in great lakes precipitation and ambient Air, *Environ. Sci. Technol.*, *44*, 7764–7770.

Graydon, J. A., V. L. St Louis, H. Hintelmann, S. E. Lindberg, K. A. Sandilands, J. W. M. Rudd, C. A. Kelly, M. T. Tate, D. P. Krabbenhoft, and I. Lehnherr (2009), Investigation of uptake and retention of atmospheric Hg(II) by boreal forest plants using stable Hg isotopes, *Environ. Sci. Technol.*, *43*, 4960–4966.

Graydon, J. A., V. L. St Louis, S. E. Lindberg, H. Hintelmann, and D. P. Krabbenhoft (2006), Investigation of mercury exchange between forest canopy vegetation and the atmosphere using a new dynamic chamber, *Environ. Sci. Technol.*, *40*, 4680–4688.

Grigal, D. F. (2003. Mercury sequestration in forests and peatlands: a review, *J. Environ. Qual.*, *32*, 393–405.

Grigal, D. F., R. K. Kolka, J. A. Fleck, and E. A. Nater (2000), Mercury budget of an upland-peatland watershed, *Biogeochemistry*, *50*, 95–109.

Gustin, M. S., H. Biester, and C. S. Kim (2002), Investigation of the light-enhanced emission of mercury from naturally enriched substrates, *Atmos. Environ.*, *36*, 3241–3254.

Gustin, M. S., M. F. Coolbaugh, M. A. Engle, B. C. Fitzgerald, R. E. Keislar, S. E. Lindberg, D. M. Nacht, J. Quashnick, J. J. Rytuba, C. Sladek, H. Zhang, and R. E. Zehner (2003), Atmospheric mercury emissions from mine wastes and surrounding geologically enriched terrains, *Environ. Geol.*, *43*, 339–351.

Gustin, M. S., M. Engle, J. Ericksen, S. Lyman, J. Stamenkovic, and M. Xin (2006), Mercury exchange between the atmosphere and low mercury containing substrates, *Appl. Geochem.*, *21*, 1913–1923.

Gustin, M. S., J. A. Ericksen, D. E. Schorran, D. W. Johnson, S. E. Lindberg, and J. S. Coleman (2004), Application of controlled mesocosms for understanding mercury air-soil-plant exchange, *Environ. Sci. Technol.*, *38*, 6044–6050.

Gustin, M. S., et al. (1999), Nevada STORMS project: Measurement of mercury emissions from naturally enriched surfaces, *J. Geophys. Res.-Atmospheres*, *104*, 21831–21844.

Gustin, M. S., S. E. Lindberg, and P. J. Weisberg (2008), An update on the natural sources and sinks of atmospheric mercury, *Appl. Geochem.*, *23*, 482–493.

Hall, B. D., and V. L. St. Louis (2004), Methylmercury and total mercury in plant litter decomposing in upland forests and flooded landscapes, *Environ. Sci. Technol.*, *38*, 5010–5021.

Hedgecock, I. M., and N. Pirrone (2004), Chasing quicksilver: modeling the atmospheric lifetime of Hg-(g)(0) in the marine boundary layer at various latitudes, *Environ. Sci. Technol.*, *38*, 69–76.

Hintelmann, H., R. Harris, A. Heyes, J. P. Hurley, C. A. Kelly, D. P. Krabbenhoft, S. Lindberg, J. W. M. Rudd, K. J. Scott, and V. L. St Louis (2002), Reactivity and mobility of new and old mercury deposition in a Boreal forest ecosystem during the first year of the METAALICUS study, *Environ. Sci. Technol.*, *36*, 5034–5040.

Hofmockel, K. S., D. R. Zak, K. K. Moran, and J. D. Jastrow (2011), Changes in forest soil organic matter pools after a decade of elevated CO(2) and O(3), *Soil Biol. Biochem.*, *43*, 1518–1527.

Iverfeldt, A. (1991), Mercury in Forest Canopy Throughfall Water and Its Relation to atmospheric deposition, *Water Air Soil Pollut.*, *56*, 553–564.

Jackson, T. A., D. M. Whittle, M. S. Evans, and D. C. G. Muir (2008), Evidence for mass-independent and mass-dependent fractionation of the stable isotopes of mercury by natural processes in aquatic ecosystems, *Appl. Geochem.*, *23*, 547–571.

Karnosky, D. F., Z. E. Gagnon, R. E. Dickson, M. D. Coleman, E. H. Lee, and J. G. Isebrands (1996a), Changes in growth, leaf abscission, and biomass associated with seasonal tropospheric ozone exposures of populus tremuloides clones and seedlings, *Can. J. For. Res.-Revue Canadienne De Recherche Forestiere*, *26*, 23–37.

Karnosky, D. F., Z. Gagnon, R. E. Dickson, P. Pechter, M. Coleman, O. Kull, A. Sober, and J. G. Isebrands (1996b), Effects of ozone and CO2 on the growth and physiology of aspen. Pages 21-21 *in* 1995 meeting of the northern global change program, Proceedings.

Karnosky, D. F., et al. (2003), Tropospheric O-3 moderates responses of temperate hardwood forests to elevated CO2: a synthesis of molecular to ecosystem results from the Aspen FACE project, *Funct. Ecol.*, *17*, 289–304.

Keeler, G., G. Glinsorn, and N. Pirrone (1995), Particulate Mercury in the Atmosphere - Its significance, transport, transformation and sources, *Water Air Soil Pollut.*, *80*, 159–168.

King, J. S., M. E. Kubiske, K. S. Pregitzer, G. R. Hendrey, E. P. McDonald, C. P. Giardina, V. S. Quinn, and D. F. Karnosky (2005), Tropospheric O-3 compromises net primary production in young stands of trembling aspen, paper birch and sugar maple in response to elevated atmospheric CO2, *New Phytol.*, *168*, 623–635.

Kolka, R. K., D. F. Grigal, E. S. Verry, and E. A. Nater (1999a), Mercury and organic carbon relationships in streams draining forested upland peatland watersheds, *J. Environ. Qual.*, *28*, 766–775.

Kolka, R. K., E. A. Nater, D. F. Grigal, and E. S. Verry (1999b), Atmospheric inputs of mercury and organic carbon into a forested upland bog watershed, *Water Air Soil Pollut.*, *113*, 273–294.

Kolka, R. K., D. F. Grigal, E. A. Nater, and E. S. Verry (2001), Hydrologic cycling of mercury and organic carbon in a forested upland-bog watershed, *Soil Sci. Soc. Am. J.*, *65*, 897–905.

Kritee, K., T. Barkay, and J. D. Blum (2009), Mass dependent stable isotope fractionation of mercury during mer mediated microbial degradation of monomethylmercury, *Geochim. Cosmochim. Acta*, *73*, 1285–1296.

Kritee, K., J. D. Blum, and T. Barkay (2008), Mercury stable isotope fractionation during Reduction of Hg(II) by different microbial pathways, *Environ. Sci. Technol.*, *42*, 9171–9177.

Kritee, K., J. D. Blum, M. W. Johnson, B. A. Bergquist, and T. Barkay (2007), Mercury stable isotope fractionation during reduction of Hg(II) to Hg(0) by mercury resistant microorganisms, *Environ. Sci. Technol.*, *41*, 1889–1895.

Kubiske, M. E., K. S. Pregitzer, D. R. Zak, and C. J. Mikan (1998), Growth and C allocation of populus tremuloides genotypes in response to atmospheric CO2 and soil N availability, *New Phytol.*, *140*, 251–260.

Kuiken, T., M. Gustin, H. Zhang, S. Lindberg, and B. Sedinger (2008a), Mercury emission from terrestrial background surfaces in the eastern USA. II: Air/surface exchange of mercury within forests from south Carolina to new England, *Appl. Geochem.*, *23*, 356–368.

Kuiken, T., H. Zhang, M. Gustin, and S. Lindberg (2008b), Mercury emission from terrestrial background surfaces in the eastern USA. Part I: Air/surface exchange of mercury within a southeastern deciduous forest (Tennessee) over one year, *Appl. Geochem.*, *23*, 345–355.

Landis, M. S., and G. J. Keeler (1997), Critical evaluation of a modified automatic wet-only precipitation collector for mercury and trace element determinations, *Environ. Sci. Technol.*, *31*, 2610–2615.

Lauretta, D. S., B. Klaue, J. D. Blum, and P. R. Buseck (2001), Mercury abundances and isotopic compositions in the Murchison (CM) and Allende (CV) carbonaceous chondrites, *Geochim. Cosmochim. Acta*, *65*, 2807–2818.

Lefticariu, L., J. D. Blum, and J. D. Gleason (2010), Mercury isotopes in Illinois basin coal: organic and inorganic constituents, *Geochim. Cosmochim. Acta*, *74*, A577–A577.

Lefticariu, L., J. D. Blum, and J. D. Gleason (2011), Mercury isotopic evidence for multiple mercury sources in Coal from the Illinois basin, *Environ. Sci. Technol.*, *45*, 1724–1729.

Lindberg, S. E. (1996), Forests and the global biogeochemical cycle of mercury: the importance of understanding air/vegetation exchange processes. Pages 359-380 *in* global and regional mercury dycles: sources, fluxes and mass balances.

Lindberg, S. E., and W. J. Stratton (1998), Atmospheric mercury speciation: Concentrations and behavior of reactive gaseous mercury in ambient air, *Environ. Sci. Technol.*, *32*, 49–57.

Lindberg, S. E., et al. (1999), Increases in mercury emissions from desert soils in response to rainfall and irrigation, *J. Geophys. Res.-Atmos.*, *104*, 21,879–21,888.

Lindberg, S. E., H. Zhang, A. F. Vette, M. S. Gustin, M. O. Barnett, and T. Kuiken (2002), Dynamic flux chamber measurement of gaseous mercury emission fluxes over soils: Part 2 - effect of flushing flow rate and verification of a two-resistance exchange interface simulation model, *Atmos. Environ.*, *36*, 847–859.

Lyman, S. N., M. S. Gustin, E. M. Prestbo, and F. J. Marsik (2007), Estimation of dry deposition of atmospheric mercury in Nevada by direct and indirect methods, *Environ. Sci. Technol.*, *41*, 1970–1976.

Mason, R. P., and G. R. Sheu (2002), Role of the ocean in the global mercury cycle, *Global Biogeochem. Cycles*, *16*(4), 40–1 to 40–14, doi:10.1029/2001GB001440.

Mauclair, C., J. Layshock, and A. Carpi (2008), Quantifying the effect of humic matter on the emission of mercury from artificial soil surfaces, *Appl. Geochem.*, *23*, 594–601.

Meili, M. (1991), The Coupling of mercury and organic-matter in the biogeochemical cycle - towards a mechanistic model for the boreal forest zone, *Water Air Soil Pollut.*, *56*, 333–347.

Mierle, G., and R. Ingram (1991), The Role of Humic Substances in the Mobilization of mercury from watersheds, *Water Air Soil Pollut.*, *56*, 349–357.

Millhollen, A. G., M. S. Gustin, and D. Obrist (2006a), Foliar mercury accumulation and exchange for three tree species, *Environ. Sci. Technol.*, *40*, 6001–6006.

Millhollen, A. G., D. Obrist, and M. S. Gustin (2006b), Mercury accumulation in grass and forb species as a function of atmospheric carbon dioxide concentrations and mercury exposures in air and soil, *Chemosphere*, *65*, 889–897.

Moore, C., and A. Carpi (2005), Mechanisms of the emission of mercury from soil: Role of UV radiation, *J. Geophys. Res.-Atmos.*, *110*, D24302, doi:10.1029/2004JD005567.

Mosbaek, H., J. C. Tjell, and T. Sevel (1988), Plant uptake of airborne mercury in background areas, *Chemosphere*, *17*, 1227–1236.

Mowat, L. D., V. L. St Louis, J. A. Graydon, and I. Lehnherr (2011), Influence of forest canopies on the deposition of methylmercury to boreal ecosystem watersheds, *Environ. Sci. Technol.*, *45*, 5178–5185.

Mulak, T., S. M. Landhausser, and V. J. Lieffers (2006), Effects of timing of cleaning and residual density on regeneration of juvenile aspen stands, *For. Ecol. Manage.*, *232*, 198–204.

Nacht, D. M., and M. S. Gustin (2004), Mercury emissions from background and altered geologic units throughout Nevada, *Water Air Soil Pollut.*, *151*, 179–193.

Natali, S. M., S. A. Sanudo-Wilhelmy, R. J. Norby, H. Zhang, A. C. Finzi, and M. T. Lerdau (2008), Increased mercury in forest soils under elevated carbon dioxide, *Oecologia*, *158*, 343–354.

Nater, E. A., and D. F. Grigal (1992), Regional trends in mercury distribution across the great-lakes states, north central USA, *Nature*, *358*, 139–141.

Point, D., J. E. Sonke, R. D. Day, D. G. Roseneau, K. A. Hobson, S. S. Vander Pol, A. J. Moors, R. S. Pugh, O. F. X. Donard, and P. R. Becker (2011), Methylmercury photodegradation influenced by sea-ice cover in arctic marine ecosystems, *Nature Geosci.*, *4*, 188–194.

Rasmussen, P. E., G. C. Edwards, R. J. Kemp, C. R. Fitzgerald-Hubble, and W. H. Schroeder (1998), Towards an improved natural sources inventory for mercury. Pages 73–83 *in* metals and the environment.

Rea, A. W., G. J. Keeler, and T. Scherbatskoy (1995), The Deposition of Mercury in throughfall and litterfall in a northern mixed hardwood forest. Abstracts of Papers of the American Chemical Society 210:75–GEOC.

Rea, A. W., G. J. Keeler, and T. Scherbatskoy (1996), The deposition of mercury in throughfall and litterfall in the lake champlain watershed: a short-term study, *Atmos. Environ.*, *30*, 3257–3263.

Rea, A. W., S. E. Lindberg, and G. J. Keeler (2000), Assessment of dry deposition and foliar leaching of mercury and selected trace elements based on washed foliar and surrogate surfaces, *Environ. Sci. Technol.*, *34*, 2418–2425.

Rea, A. W., S. E. Lindberg, and G. J. Keeler (2001), Dry deposition and foliar leaching of mercury and selected trace elements in deciduous forest throughfall, *Atmos. Environ.*, *35*, 3453–3462.

Rea, A. W., S. E. Lindberg, T. Scherbatskoy, and G. J. Keeler (2002), Mercury accumulation in foliage over time in two northern mixed-hardwood forests, *Water Air Soil Pollut.*, *133*, 49–67.

Rutter, A. P., J. J. Schauer, M. M. Shafer, J. E. Creswell, M. R. Olson, M. Robinson, R. M. Collins, A. M. Parman, T. L. Katzman, and J. L. Mallek (2011), Dry deposition of gaseous elemental mercury to plants and soils using mercury stable isotopes in a controlled environment, *Atmos. Environ.*, *45*, 848–855.

Schauble, E. A. (2007. Role of nuclear volume in driving equilibrium stable isotope fractionation of mercury, thallium, and other very heavy elements, *Geochim. Cosmochim. Acta*, *71*, 2170–2189.

Schroeder, W. H., and J. Munthe (1998), Atmospheric mercury - an overview, *Atmos. Environ.*, *32*, 809–822.

Schroeder, W. H., S. Beauchamp, G. Edwards, L. Poissant, P. Rasmussen, R. Tordon, G. Dias, J. Kemp, B. Van Heyst, and C. M. Banic (2005), Gaseous mercury emissions from natural sources in Canadian landscapes, *J. Geophys. Res.-Atmos.*, *110*, D18302, doi:10.1029/2004JD005699.

Schuster, E. (1991. The behavior of mercury in the soil with special emphasis on complexation and adsorption processes - a review of the literature, *Water Air Soil Pollut.*, *56*, 667–680.

Sellers, P., C. A. Kelly, J. W. M. Rudd, and A. R. MacHutchon (1996), Photodegradation of methylmercury in lakes, *Nature*, *380*, 694–697.

Senn, D. B., E. J. Chesney, J. D. Blum, M. S. Bank, A. Maage, and J. P. Shine (2010), stable isotope (N, C, Hg) study of methylmercury sources and trophic transfer in the northern gulf of Mexico, *Environ. Sci. Technol.*, *44*, 1630–1637.

Shanley, J. B., P. F. Schuster, M. M. Reddy, D. A. Roth, H. E. Taylor, and G. R. Aiken (2002), Mercury on the move during snowmelt in Vermont, *Eos Trans. AGU*, *83*, 45–48.

Sherman, L. S., J. D. Blum, K. P. Johnson, G. J. Keeler, J. A. Barres, and T. A. Douglas (2010), Mass-independent fractionation of mercury isotopes in Arctic snow driven by sunlight, *Nature Geosci.*, *3*, 173–177.

Sherman, L. S., J. D. Blum, G. J. Keeler, J. D. Demers, and J. T. Dvonch (2012), Investigation of local mercury deposition from a coal-fired power plant using mercury isotopes, *Environ. Sci. Technol.*, *46*, 382–390.

Sherman, L. S., J. D. Blum, D. K. Nordstrom, R. B. McCleskey, T. Barkay, and C. Vetriani (2009), Mercury isotopic composition of hydrothermal systems in the Yellowstone Plateau volcanic field and Guaymas basin sea-floor rift, *Earth Planet. Sci. Lett.*, *279*, 86–96.

Shi, W. F., X. B. Feng, G. Zhang, L. L. Ming, R. S. Yin, Z. Q. Zhao, and J. Wang (2011), High-precision measurement of mercury isotope ratios of atmospheric deposition over the past 150 years recorded in a peat core taken from Hongyuan, Sichuan province, China, *Chinese Sci. Bull.*, *56*, 877–882.

Smith, C. N., S. E. Kesler, J. D. Blum, and J. J. Rytuba (2008), Isotope geochemistry of mercury in source rocks, mineral deposits and spring deposits of the California coast ranges, USA, *Earth Planet. Sci. Lett.*, *269*, 398–406.

Smith, C. N., S. E. Kesler, B. Klaue, and J. D. Blum (2005), Mercury isotope fractionation in fossil hydrothermal systems, *Geology*, *33*, 825–828.

Sonke, J. E. (2011), A global model of mass independent mercury stable isotope fractionation. *Geochim. Cosmochim. Acta*, doi:10.1016/j.gca.2011.05.027.

Sonke, J. E., O. Pokrovsky, and V. Schevchenko (2011), Mercury stable isotopic compositions of lichens and mosses from the Russian (sub-)arctic. The 10th International conference on mercury as a global pollutant. Halifax, Nova Scotia, Canada.

St. Louis, V. L., J. W. M. Rudd, C. A. Kelly, B. D. Hall, K. R. Rolfhus, K. J. Scott, S. E. Lindberg, and W. Dong (2001), Importance of the forest canopy to fluxes of methyl mercury and total mercury to boreal ecosystems, *Environ. Sci. Technol.*, *35*, 3089–3098.

Stamenkovic, J., and M. S. Gustin (2009), Nonstomatal versus Stomatal Uptake of Atmospheric Mercury, *Environ. Sci. Technol.*, *43*, 1367–1372.

Talhelm, A. F., K. S. Pregitzer, and D. R. Zak (2009), Species-specific responses to atmospheric carbon dioxide and tropospheric ozone mediate changes in soil carbon, *Ecol. Lett.*, *12*, 1219–1228.

Urey, H. C. (1947. The Thermodynamic Properties of isotopic substances, *J. Chem. Soc.*:562–581.

USEPA (1998), Method 1631: Measurement of mercury in water; revision E. U.S. Environmental protection agency, office of water, office of science and technology, engineering and analysis division (4303), Washington, D.C., USA.

Wallschlager, D., R. R. Turner, J. London, R. Ebinghaus, H. H. Kock, J. Sommar, and Z. F. Xiao (1999), Factors affecting the measurement of mercury emissions from soils with flux chambers, *J. Geophys. Res.-Atmospheres*, *104*, 21859–21871.

Wiederhold, J. G., C. J. Cramer, K. Daniel, I. Infante, B. Bourdon, and R. Kretzschmar (2010), Equilibrium mercury isotope fractionation between dissolved Hg(II) species and thiol-bound Hg, *Environ. Sci. Technol.*, *44*, 4191–4197.

Xin, M., and M. S. Gustin (2007), Gaseous elemental mercury exchange with low mercury containing soils: investigation of controlling factors, *Appl. Geochem.*, *22*, 1451–1466.

Xin, M., M. Gustin, and D. Johnson (2007), Laboratory investigation of the potential for re-emission of atmospherically derived Hg from soils, *Environ. Sci. Technol.*, *41*, 4946–4951.

Yin, Y. J., H. E. Allen, C. P. Huang, and P. F. Sanders (1997), Interaction of Hg(II) with soil-derived humic substances, *Anal. Chim. Acta*, *341*, 73–82.

Zak, D. R., W. E. Holmes, K. S. Pregitzer, J. S. King, D. S. Ellsworth, and M. E. Kubiske (2007), Belowground competition and the response of

developing forest communities to atmospheric CO2 and O-3, *Global Change Biol.*, *13*, 2230–2238.

Zambardi, T., J. E. Sonke, J. P. Toutain, F. Sortino, and H. Shinohara (2009), Mercury emissions and stable isotopic compositions at vulcano island (Italy), *Earth Planet. Sci. Lett.*, *277*, 236–243.

Zhang, H., and S. E. Lindberg (1999), Processes influencing the emission of mercury from soils: A conceptual model, *J. Geophys. Res.-Atmospheres*, *104*, 21889–21896.

Zhang, H., S. E. Lindberg, and M. S. Gustin (2001), Nature of diel trend of mercury emission from soil: Current understanding and hypotheses. Abstracts of papers of the American chemical society 222:67–ENVR.

Zheng, W., and H. Hintelmann (2009), Mercury isotope fractionation during photoreduction in natural water is controlled by its Hg/DOC ratio, *Geochim. Cosmochim. Acta*, *73*, 6704–6715.

Zheng, W., and H. Hintelmann (2010a), Isotope fractionation of mercury during Its photochemical reduction by low-molecular-weight organic compounds, *J. Phys. Chem. A*, *114*, 4246–4253.

Zheng, W., and H. Hintelmann (2010b), Nuclear field shift effect in isotope fractionation of mercury during abiotic reduction in the absence of light, *J. Phys. Chem. A*, *114*, 4238–4245.

Zheng, W., D. Foucher, and H. Hintelmann (2007), Mercury isotope fractionation during volatilization of Hg(0) from solution into the gas phase, *J. Anal. Atom. Spectrom.*, *22*, 1097–1104.